Ce^{3+} Ion Activated Fluoride Crystals as Prospective Active Media for High-Power All-Solid-State Ultraviolet Tunable Ultrafast Lasers

A dissertation submitted for the degree of
Doctor of Philosophy

by

Zhenlin LIU

Department of Structural Molecular Science
The Graduate University for Advanced Studies

1999

Contents

Chapter 1. Introduction

The ultraviolet (UV) tunable lasers become the most important tool in many fields of science and technology. The most impressive applications include environmental sensing, engine combustion diagnostics, semiconductor processing, micromaching, optical communications, and medicinal and biological applications.

For example, the behavior of trace constituents in the earth's upper atmosphere, governed by chemical, dynamical, and radiative processes, is of particular importance for the overall balance of the stratosphere and mesosphere. In particular ozone plays a dominant role by absorbing the short-wavelength UV radiation which might damage living organisms and by maintaining the radiative budget equilibrium. The measurement of the total ozone column content and vertical profile by a ground-based UV spectrometer network or by satellite-borne systems remains the fundamental basis for global observations and trend analysis. Remote measurements of the trace constituents using an active technique such as lidar have been made possible by the rapid development of powerful tunable laser sources which have opened a new field in atmospheric spectroscopy by providing sources which can be tuned to characteristic spectral features of atmospheric constituents [1].

Recently, NASA missions used tunable UV laser sources for atmospheric differential absorption lidar (DIAL) measurements from the airplanes to analyze the global distribution of O_3 radicals which is directly relevant to the "ozone hole" and global climate formation problems [2]. In the airborne UV DIAL system, two frequency-doubled Nd:YAG lasers are used to pump two high-conversion-efficiency, frequency-doubled, tunable dye lasers. They used the UV lasers in the wavelength region from 289 to 311 nm.

1.1 Present situation of UV laser systems

Considerable effort has been devoted since the early 1970s to the development of new vibronic crystals for tunable solid-state lasers. However, almost all the efficient and successful vibronic materials, like Ti:sapphire [3], Alexandrite [4], and more recently Cr^{3+}:$LiCaAlF_6$ (Cr:LiCAF) [5] and Cr^{3+}:$LiSrAlF_6$ (Cr:LiSAF) [6] are emitting in the same near-IR spectral region (700-1000 nm).

1.1.1 UV laser systems using frequency conversion

The existing commercially available tunable UV laser sources (comprising subsequent steps of nonlinear frequency conversion - doubling, tripling and/or mixing of tunable radiation obtained from the primary traditional tunable visible or near infrared lasers) are extremely complicated and expensive (also bulky, inefficient, inconvenient, and unreliable for airborne measurements in flight or aboard spacecraft applications, as emphasized in ref. 2) up to now. For example, UV tunable lasers based on dye-laser tunability, in addition to a pumping source (usually an Ar^+ ion laser or an Nd:YAG laser with an attached nonlinear frequency-doubler), need a tunable dye laser in the orange-red region of the spectrum, which should be provided with a dye circulation system as well as a system for frequency-doubling of the dye laser radiation with a servo-tuning system (often called "Autotracker") to follow the wavelength changes and also a system for separation of the visible and UV beams emanating from it. Solid-state tunable UV lasers using Ti:sapphire lasers with subsequent mixing of its tunable output with 532-nm pumping radiation should also be supplied by "Autotracker" [7].

Recent development of frequency-tripled flash lamp-pumped Q-switched Cr:LiSAF tunable laser holds promise for devising more reliable tunable solid-state UV lasers. Cr:LiSAF is of particular interest due to its strong absorption in the 670 nm wavelength region, allowing for potential pumping with AlGaInP/GaAs diode lasers. The schematic diagram of the tunable all-solid-

state UV laser is shown in Fig. 1.1. The harmonic generation in the UV region from 260 to 320 nm was demonstrated using an LBO/BBO sum-frequency mixing scheme. The maximum output was 6 mJ at the wavelength of 300 nm [8].

On the other hand, remarkable progress in high-power ultrashort pulse lasers has been made since chirped-pulse amplification [9] was applied to solid-state lasers such as Ti:sapphire lasers along with the generation of ultrashort pulses. These success, however, did not extend to UV-wavelength region, because the frequency upconversion limits the bandwidth, resulting in a long pulse width and low conversion efficiency. For higher peak power or high average power in the UV region, UV gain media with broad gain bandwidth are necessary.

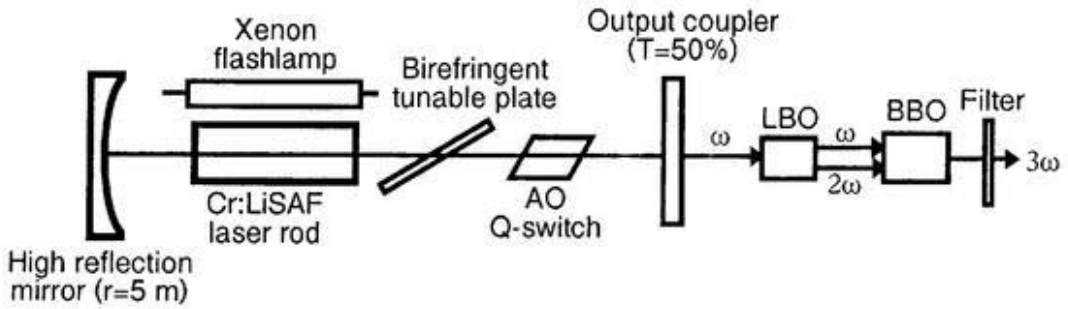

Fig. 1.1 Schematic diagram of the tunable all-solid-state UV laser [8].

1.1.2 Direct generation of UV coherent light from lasers

To provide tunable or ultrashort UV laser radiation in a reliable and efficient way, the most prospective version at the moment would be to use directly-pumped solid-state UV active media, based on the electrically-dipole-allowed interconfigurational 5d-4f transitions of rare-earth ions in wide band-gap fluoride crystals: $YLiF_4$ (YLF) [10], LaF_3 [11] and more recently $LuLiF_4$ (LLF) [12,13], $LiCaAlF_6$ (LiCAF) [14-16], and $LiSrAlF_6$ (LiSAF) [17,18]. In fact, this is the only version which also allows independent control of tunable

radiation bandwidth, or when necessary, even provides multi-wavelength UV output in one laser beam from the oscillator [12,13]. This version was proposed in 1977 from purely spectroscopic considerations [19] and then confirmed experimentally on Ce^{3+} ion in UV region by D. J. Ehrlich et al [10,11] and Nd^{3+} ion in VUV region by R. W. Waynant [20].

As early as 1977, K. H. Yang and J. A. Deluca proposed a simple way of implementing a tunable laser capable of producing radiation directly in the UV and even VUV spectral ranges [19]. For this purpose, they proposed to use interconfiguration 5d-4f transitions of rare-earth ions in wide band-gap dielectric crystals. Because of the strong lattice interaction with 5d electrons, the fluorescence that results from 5d to 4f transitions of trivalent rare-earth ions in solid hosts is characterized by broad bandwidths and large Stokes shifts. Such fluorescence is particularly attractive for the development of tunable lasers. Powder samples of Ce^{3+}:LaF_3 and Ce^{3+}:LuF_3 were excited by the 253.7-nm radiation transmitted through a narrow-band interference filter inserted in front of a Hg lamp source. Broad-band UV fluorescence were reported for Ce^{3+}:LaF_3 (276-312 nm) and Ce^{3+}:LuF_3 (288-322 nm). The fluorescence quantum yields accounts for the fact that not all of the atoms raised to the pump bands subsequently decay to the upper laser level. Some of these atoms can in fact decay from the pump bands straight back to the ground state or perhaps to other levels which are not useful. The pump quantum efficiency or fluorescence quantum yields $\eta_q(\lambda)$ is defined as the ratio of the number of atoms which decay to the upper laser level to the number of atoms which are raised to the pump band by a monochromatic pump at wavelength λ. The fluorescence quantum yields of LaF_3:1%Ce^{3+} and LuF_3:0.1%Ce^{3+} are 0.9 and 0.82, respectively. Estimates of the threshold power for lasing action suggested that a laser system tunable from 276 to 322 nm is feasible with noble-gas-halide lasers as pumping sources [19].

After that, Ce^{3+}:$Y_3Al_5O_{12}$ (YAG) was investigated as a model system for a 5d-4f solid-state tunable laser [21]. This system was chosen since YAG had been extensively studied as a laser host and good quality crystals were readily available. Despite providing apparently adequate conditions to achieve stimulated emission, it was unable to detect laser action in Ce^{3+}:YAG. It was found that there was strong excited-state absorption (ESA) in this material at the wavelengths of its fluorescence. The ESA was sufficiently strong to completely quench any possible laser action. The crystal showed a net optical loss instead of optical gain at the wavelength of the fluorescence transition. This self-absorption may explain the failure of all attempts to obtain stimulated emission in this material.

A laser of the type which has a 5d-4f transition was originally implemented with Ce^{3+}:$YLiF_4$ (Ce:YLF) as a laser medium [10]. It should be noted that Ce^{3+} ions are the most promising activators for the UV spectral range. However, in spite of a large number of studied Ce-activated materials [22,23], the investigations performed before 1992 revealed only two laser-active media [10,11].

In 1979, D. J. Ehrlich et. al. reported the first observation of stimulated emission from a 5d-4f transition in triply ionized rare earth-doped crystal Ce:YLF, optically pumped at 249 nm, and emitted at 325.5 nm [10]. Since the Ce^{3+} ion has only one electron in the 4f state, the impurity energy levels of Ce-doped crystals are particularly simple. The ground state is split into a $^2F_{5/2}$ and a $^2F_{7/2}$ levels by the spin-orbit interaction. The first excited state is a 5d state, which interacts strongly with the host lattice because of the large spatial extent of the 5d wave function. Thus the crystal-field interaction dominates over the spin-orbit interaction and the 5d state splits into four levels as a result of the S_4 site symmetry for the rare-earth ion in YLF. Figure 1.2 shows the absorption and fluorescence spectra for Ce:YLF.

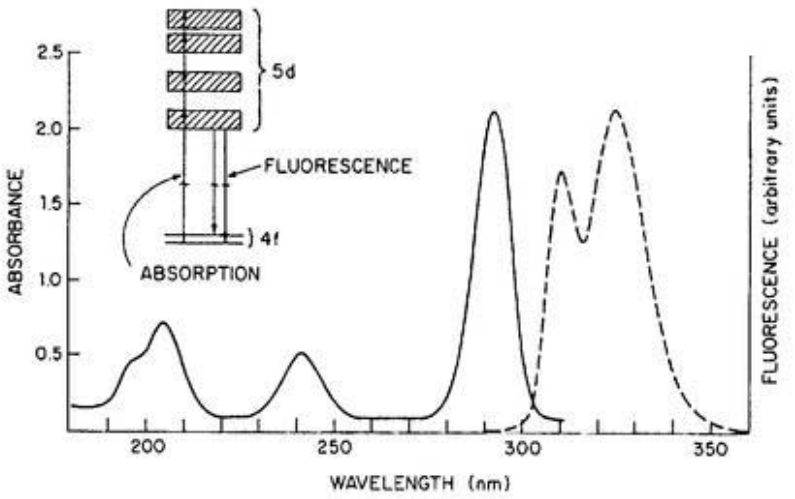

Fig. 1.2 Absorption (solid line) and fluorescence (dot line) spectra of Ce:YLF [10].

The broad absorption bands that peak at 195, 205, 240, and 290 nm result from transitions from the 4f ground state to the crystal-field split 5d levels of the Ce^{3+} ion. The fluorescence spectrum has two peaks, the result of transitions from the lowest 5d level to the two spin-orbit ground states $4f(^2F_{5/2})$ and $4f(^2F_{7/2})$. The 40-ns radiative lifetime of the 5d level results from the electric-dipole-allowed character of the 5d→4f transition. The potential tuning range of the Ce:YLF laser estimated from the half-power points of the fluorescence spectrum is from 305 to 335 nm. The maximum output energy observed was ~1μJ in a pulse width of 35 ns for an absorbed pump energy of 300 μJ.

However, the operation of the Ce:YLF laser is hampered by several poor performance characteristics. These include an early onset of saturation and rolloff in the above-threshold gain and power output as well as a drop in the output for pulse repetition rates above 0.5 Hz. It has been shown that an excited state absorption of the UV pump light is responsible for a photoionization of the Ce^{3+} ions, which in turn leads to the formation of transient and stable color centers. The color centers have a deleterious effect on the lasing characteristics of Ce:YLF since they absorb at the cerium emission wavelengths. The growth

and relaxation of these centers influence the gain saturation and pump rate limitation of the Ce:YLF laser [24,25]. This experiment is of historic significance, but it is short of practical use due to the existence of solarization.

In 1980, the same group mentioned above reported the operation of an optically pumped Ce^{3+}:LaF_3 laser [11]. The unpolarized near-UV absorption and emission spectra for a 0.05% Ce-doped LaF_3 crystal are shown in Fig. 1.3. Because of the rapid internal relaxation to the lowest 5d state, the fluorescence spectrum was not noticeably different for ArF (193 nm), KrF (248 nm), or frequency-doubled Ar^+ ion laser (257 nm) pumping. Similarly, the fluorescence lifetime was identical for 248-nm or 193-nm excitation. For the 0.05%-doped crystal, the lifetime was 18 ± 2 ns. The approximate potential tuning range is from 275 to 315 nm. The output of a small commercial excimer laser, producing 40 mJ at 248 nm or 10 mJ at 193 nm in a 25-ns (FWHM) pulse, was used for optical pumping. The primary difficulties encountered, i.e., low output power and high threshold, can probably be ascribed to initial difficulties in crystal growth. However, no one can repeat the result of this experiment, it is difficult to comment on the properties of Ce^{3+}:LaF_3 crystal as a laser medium.

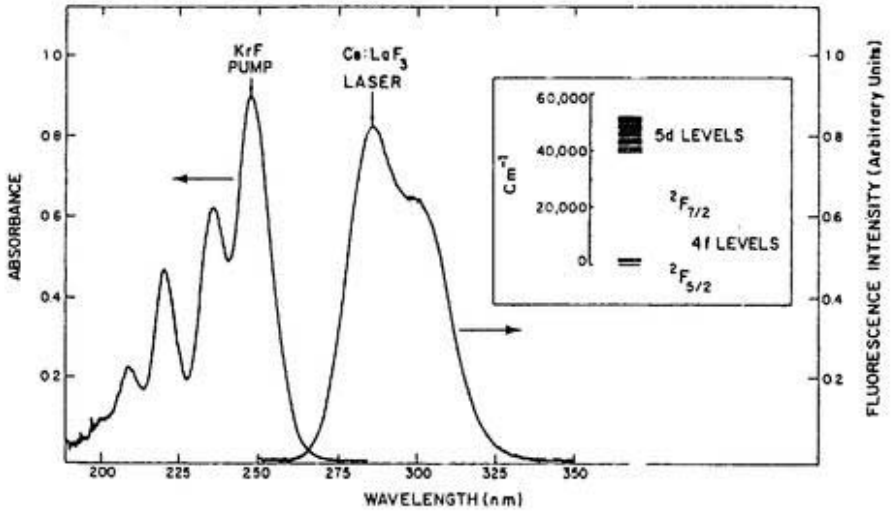

Fig. 1.3 Ultraviolet absorption and spontaneous emission of a 700-μm-thick LaF_3 crystal with 0.05 at. % Ce^{3+} ion doping [11].

Subsequent studies showed that the attempts to find laser-active media among Ce-activated materials failed because of absorption from the excited state of the 5d configuration of Ce^{3+} ions in Ce^{3+}:YAG [26, 27] and Ce^{3+}:CaF_2 [28], formation of stable or transient color centers in Ce-activated samples [23,24,28], and other complicated processes occurring in such media under the high-power UV pumping.

The spectrally broad vibronic emission bands in impurity-doped solids serve as the basis for wavelength-tunable laser operation in these materials. But because of the broad emission and absorption bands, these materials are susceptible to ESA which can significantly reduce the performance characteristics of the laser materials. The ESA is a two-step process, where the first photon absorbed promotes an electron from the 4f ground state to the lowest 5d state of the trivalent cerium ion. Within the lifetime of this excited 5d state, a second photon is absorbed which then photoionizes the ion by promoting that electron to the conduction band. The free electron subsequently traps out at an electron acceptor site forming a stable color center. These color centers are absorptive at the wavelengths for stimulated emission of the trivalent cerium ions, and hence they serve as a quenching mechanism for laser gain in this crystal. The color centers produced are photochromic in that they can be optically bleached [23]. Over a long period of time, difficulties in overcoming these problems, which are inherent in well-known materials used for producing UV light [10,11], made investigators believe that this scheme of UV lasers was of little promise.

However, recent investigations showed that, by an appropriate choice of activator-matrix complexes and active medium-pump source combinations, one can create efficient tunable lasers using d-f transitions in Ce^{3+} ion in the UV

spectral range [12-16] and in Nd^{3+} ion in the VUV range [29]. Furthermore, such lasers proved to be stable under the pumping.

In 1992, M. A. Dubinskii et al. of Russia reported UV laser medium, Ce^{3+}:$LuLiF_4$ (Ce:LLF) crystal, which can be pumped by KrF excimer laser. This crystal has almost the same optical properties with Ce:YLF. But Ce:LLF has smaller solarization effect, and it is more hopeful in practical use [12,13]. In 1993, the same group reported Ce^{3+}:$LiCaAlF_6$ (Ce:LiCAF) crystal which can be pumped by the fourth harmonic of Nd:YAG laser. No solarization effect of this crystal was observed [14-16].

Ce^{3+}:$LiSrAlF_6$ (Ce:LiSAF) crystal was reported in 1994, and it also can be pumped by the fourth harmonic of Nd:YAG laser [17,18]. It has the similar laser properties with Ce:LiCAF crystal.

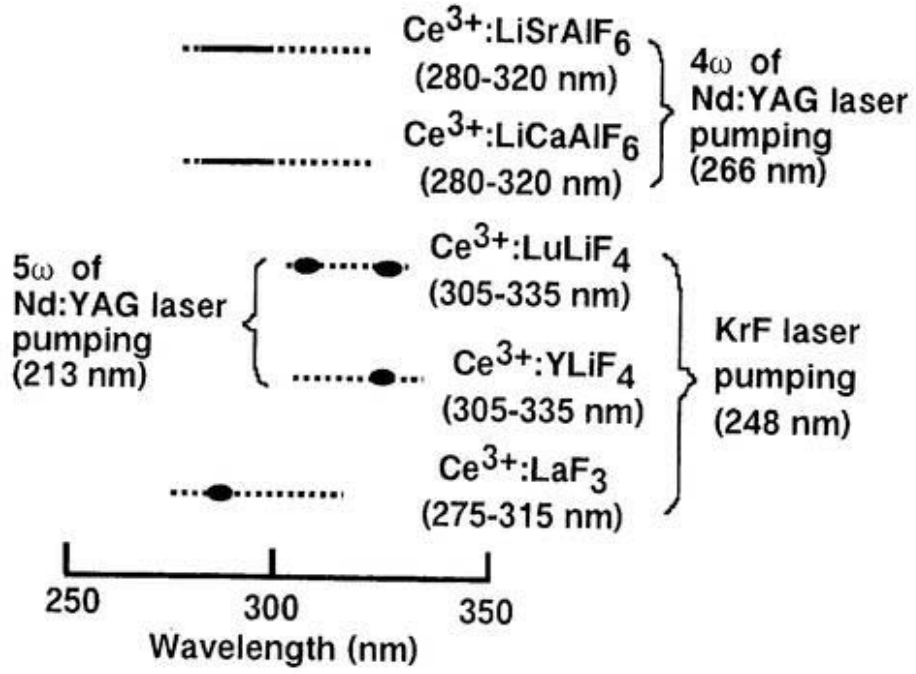

Fig. 1.4 Various tunable lasers in ultraviolet region. Solid lines and dots indicate the confirmed tunable wavelength region, dotted lines show potential tunable wavelength region.

Since these new Ce-doped crystals were reported, the studies on the ultraviolet tunable lasers have become popular again. All these new Ce-doped crystals have a broad gain-width in the ultraviolet region, which is especially attractive for ultrashort-pulse generation and amplification. Figure 1.4 shows the tunable wavelength regions of the five known Ce-doped laser crystals.

1.2 Basic properties of Ce:LLF laser medium

Ce:LLF is a tunable solid-state laser material in ultraviolet region which was first reported in 1992 by Prof. Dubinskii in Russia [10,11]. The choice of this material for the experiments in UV is more reasonable because of its structural and chemical similarity to comprehensively studied and grown commercially YLF single crystal. The LLF crystals belong to the scheelite structural type. Similar to all rare-earth ions, Ce^{3+} ions take part in activation, substituting for Lu^{3+} ions in the position with the point group S_4.

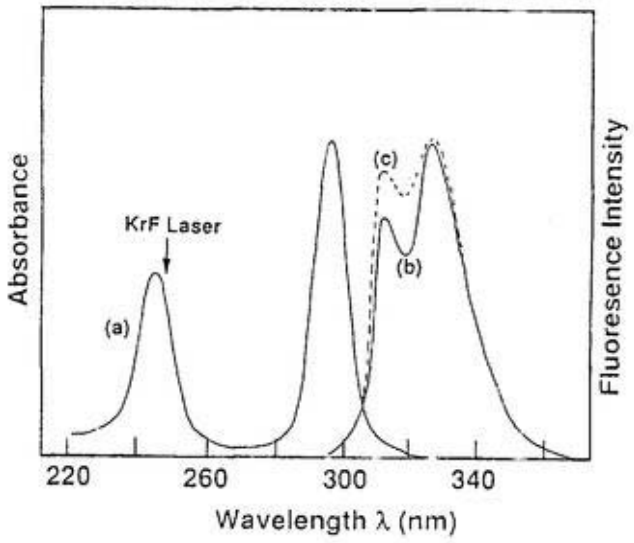

Fig. 1.5 π-polarized absorption (a) and normalized fluorescence (b: π-polarization, c: σ-polarization) spectra of Ce:LLF single crystal.

Ce:LLF has a potential tuning region of around 305 to 340 nm, so it is especially attractive for use in spectroscopy of wide band-gap semiconductors for blue laser diodes, such as GaN [30]. The fluorescence spectrum of Ce:LLF crystal has two peaks at 311 nm and 328 nm, respectively (Fig. 1.5). KrF excimer laser (248-nm) can be used as the pumping source for Ce:LLF crystal. The fluorescence lifetime was found to be about 40 ns.

In our previous work [31], we measured the gain spectrum and saturation fluence for Ce:LLF crystal.

1.2.1 Gain spectrum of Ce:LLF crystal

A Ce^{3+}:$LuLiF_4$ single crystal was grown from a carbon crucible using the Bridgman-Stockbarger method in a fluorinated atmosphere by Prof. Dubinskii, et al. A seeded crucible was used in order to obtain oriented boule. The seed orientation was such that the c-axis was perpendicular to the cylindrical axis of the crucible. The corresponding orientation of c-axis of grown crystal was checked by observing the conoscopic picture of the boule. The sample obtained contains about 0.5 at. % Ce^{3+} ions, and the concentration of the dopant was measured using Electron Spin Resonance (ESR) method similarly to ref. 32.

The sample for the amplification experiment (1 cm long and 5 mm dia.) was cut cylindrically. A flat window was polished on the side of the cylinder parallel to its axis. The end surfaces were polished parallel within 5 arcmin. The sample was oriented in such a manner that the c-axis of the crystal is parallel to the side window and perpendicular to the axis of the cylinder. The pump and probe experiment was done for measuring the gain spectrum for the 1-cm long Ce:LLF crystal under the randomly polarized KrF excimer laser excitation with side-pumping geometry (Fig. 1.6). The probe beam was the second harmonic of a tunable mode-locked DCM dye laser, which was synchronously pumped by the second harmonic of a cw mode-locked Nd:YAG laser. The tuning range of

the DCM dye laser is from 645 to 680 nm. The second harmonic of the DCM laser was generated using a LBO nonlinear crystal in type I phase-matching condition. When we changed the wavelength of the DCM dye laser, we need to rotate the LBO crystal to satisfy the phase-matching condition. The pumping source to excite Ce:LLF crystal was a conventional randomly-polarized KrF excimer laser. The pumping pulses were focused onto the side window of the Ce:LLF crystal by a cylindrical lens.

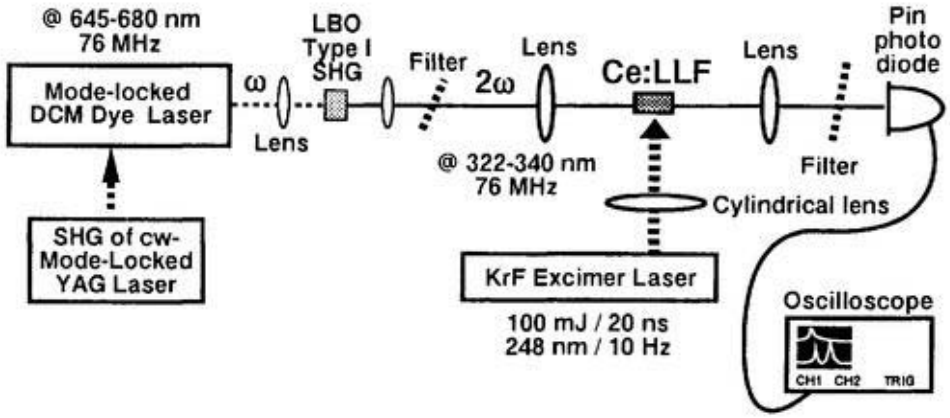

Fig. 1.6 Gain spectrum measurement using the second harmonic of a mode-locked DCM dye laser as a probe.

Figure 1.7 shows a typical oscilloscope trace of the amplification. A biplanar phototube was used to detect the signal. We used a Tektronix 7934 storage oscilloscope to display the gain traces. We took the data for two times which were with and without probe beam and saved the data on the oscilloscope screen. Then we can see the amplified pulse train and the fluorescence pulse train at the same time. The difference of the upper signal and the lower signal will be the net gain. So with the use of the mode-locked pulse train as a probe beam, the fluorescence background is easily distinguished.

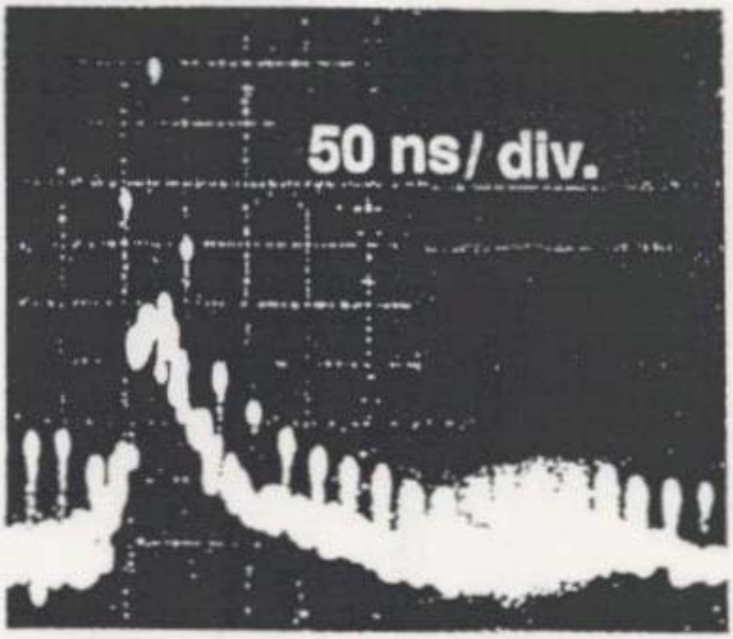

Fig. 1.7 Oscilloscope traces of the amplified pulse train (76 MHz) and the fluorescence. The gain can be easily estimated in spite of the presence of the fluorescence background.

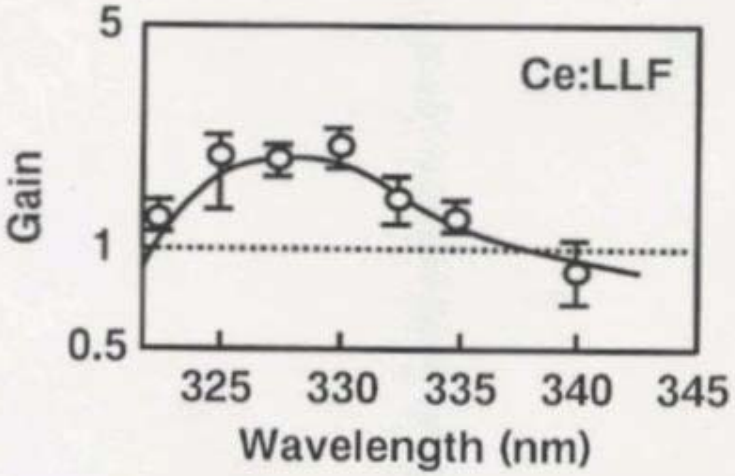

Fig. 1.8 Gain spectrum of Ce:LLF pumped by randomly-polarized KrF laser using the second harmonic of a picosecond cw mode-locked DCM dye laser as a σ-polarized probe (pumping fluence ~ 0.1 J/cm^2).

The probe beam was σ-polarized (the polarization is perpendicular to the optical axis or c axis of the Ce:LLF crystal). In order to check the gain-polarization dependence, we changed the polarization direction of the DCM dye laser by rotate a half-wave plate. No noticeable anisotropy of the gain was observed within the accuracy of our measurements (at least for 325 nm probe radiation). The gain was demonstrated from 323 nm to 335 nm (Fig. 1.8), due to the available probe laser tunability. This gain bandwidth is large enough for amplification of tunable femtosecond pulses.

1.2.2 Small-signal gain and saturation fluence of Ce:LLF crystal

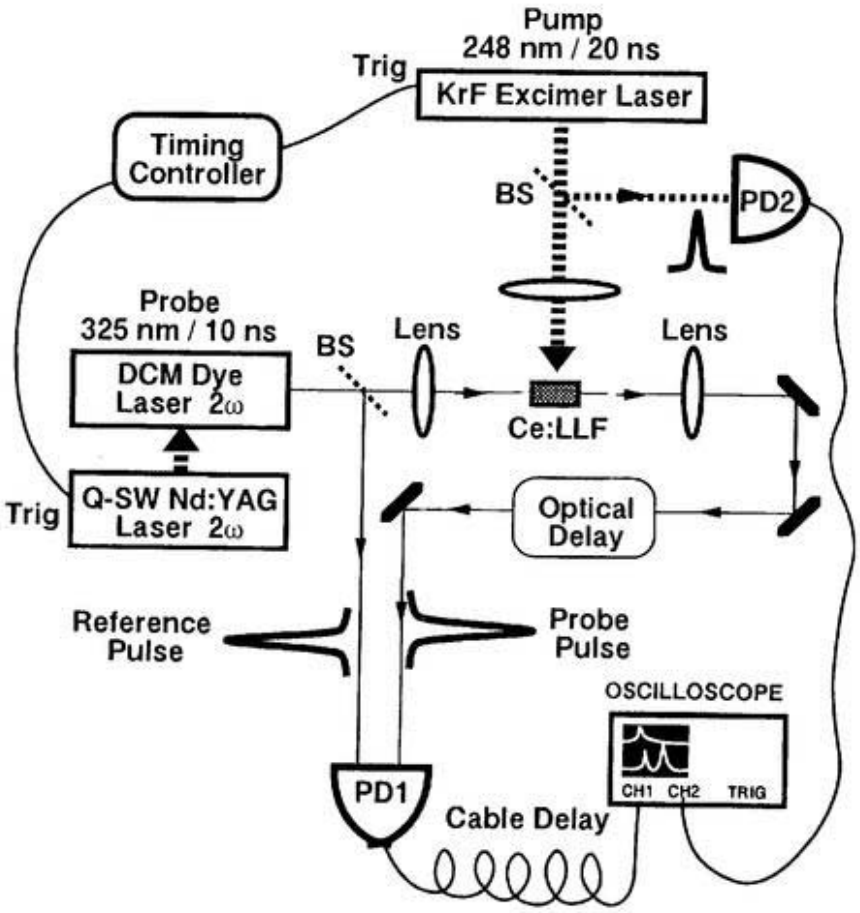

Fig. 1.9 Small-signal gain and saturation fluence were evaluated using the second harmonic (325 nm) of a nanosecond DCM-dye laser as a probe.

Small-signal gain and saturation fluence are very important parameters for designing lasers. The small-signal gain and saturation fluence of Ce:LLF were evaluated using the second harmonic (325 nm) of a nanosecond DCM-dye laser as a probe as shown in Fig. 1.9. A KrF excimer laser was used to pump the Ce:LLF from its side window. The frequency conversion scheme used LBO nonlinear crystal to double the dye laser output. The DCM dye laser was pumped by the second harmonic of a Q-switched Nd:YAG laser. The relative timing of the probe dye laser and the pumping excimer laser was controlled by a synchronizer to obtain the largest possible gain. The single-pass gain in the small-signal region (~1 mJ/cm^2) was over 6-dB/cm (4.3 times) with 0.5-J/cm^2 pumping flux (Fig. 1.10).

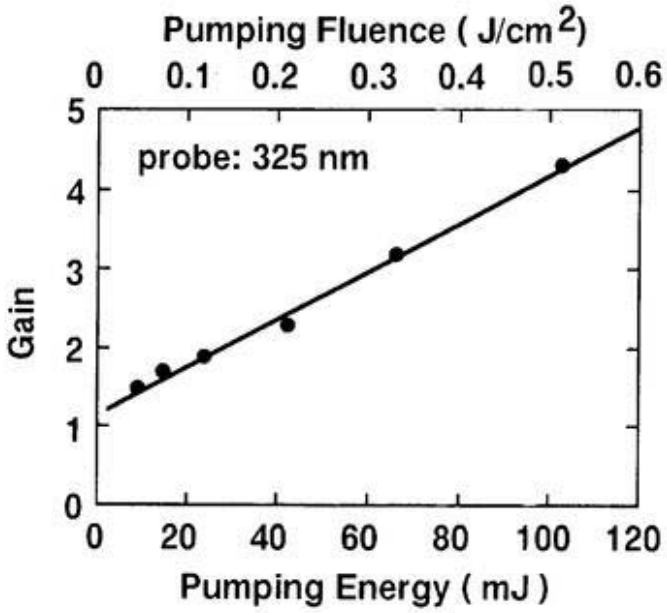

Fig. 1.10 Gain dependence of Ce:LLF on pumping power at 325 nm. The single-pass gain in the small-signal region was over 6-dB/cm (4.3 times) with 0.5-J/cm^2 excitation fluence.

The 10-ns pulsewidth of the probe light was short enough in comparison with 40-ns fluorescence lifetime of Ce:LLF, therefore the evaluation of the

saturation fluence and emission-cross section is possible under the assumption of Frantz-Nodvik relation modeled for slow-decay gain medium [33].

$$G=E_S\log_e\{1+G_o[\exp(E_i/E_S)-1]\}/E_i$$

where E_i is the input fluence, E_S is the saturation fluence, G_o is the single-pass small-signal gain, and G is the gain corresponding to E_i. The saturation fluence of Ce:LLF assuming the Frantz-Nodvik relation was estimated to be ~50 mJ/cm^2 at 325 nm (Fig. 1.11), which is about two orders of magnitude higher than that of organic dyes (~1 mJ/cm^2). The emission-cross section estimated from this saturation fluence was ~10^{-17} cm^2 by the relation of $E_S=h\nu/\sigma$. These results indicate high potential of Ce:LLF as a power amplification medium.

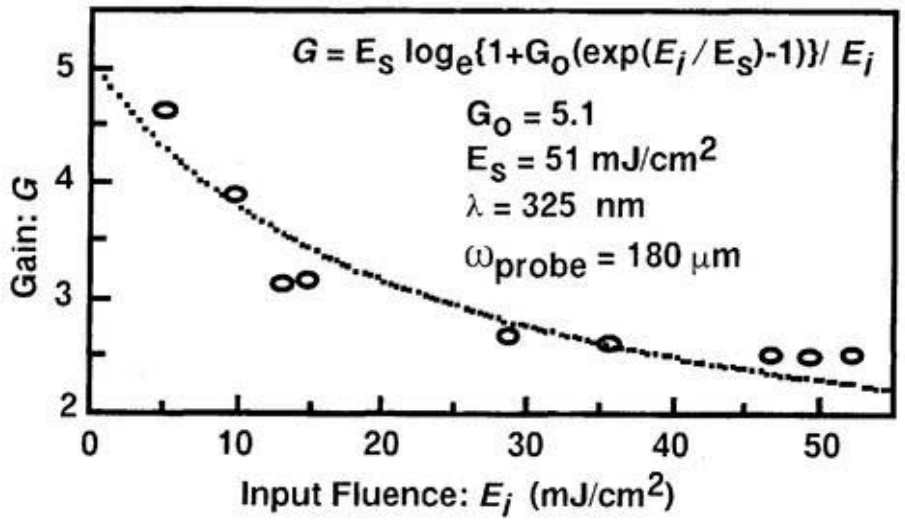

Fig. 1.11 Ce:LLF gain dependence on input fluence of 10-ns, 325-nm probe pulses. The solid line indicates the gain saturation curve assuming the Frantz-Nodvik relation, which was fitted by the least square method. The saturation fluence and the small signal gain were fitted to be 50 mJ/cm^2 and 5.1 (pumping fluence ~ 0.5 J/cm^2).

1.3 Basic properties of Ce:LiCAF laser medium

In contrast to excimer laser pumped UV solid-state laser media, such as Ce:LLF and Ce:YLF, the Ce:LiCAF crystal which was first reported by M. A.

Dubinskii et al in 1993 [14-16], is the first known tunable UV laser directly pumped by the fourth harmonic of a standard Nd:YAG laser. In that sense, this is the first truly all-solid-state tunable UV laser.

The samples of Ce:LiCAF were also grown in a fluorinated atmosphere using the Bridgeman-Stockbarger technique from carbon crucibles by Prof. Dubinskii, et al. The crystals grown had the colquiriite structure and the space group P31c. The non-polarized absorption spectrum of a 2.3 mm thick Ce:LiCAF sample, containing about 0.1% of Ce^{3+} ions, is shown in Fig. 1.12-(a). Due to the first 4f-5d-absorption peak with a half width of 3000 cm^{-1} centered at about 37,000 cm^{-1}, Ce:LiCAF can be pumped by the fourth harmonics of various commercially available Nd-lasers (e. g., YAG, YAP, YLF, and GSGG). The Ce:LiCAF fluorescence spectrum (Fig. 1.12-(b)) displays the nearly two-humped shape characteristic of Ce^{3+} ions in most known hosts, due to the allowed 5d-4f-transitions terminating at the $^2F_{7/2}$ and $^2F_{5/2}$ components of the spin-orbit split ground term. Ce:LiCAF has a potential tuning range from 280 to 320 nm. Ce:LiCAF has sufficiently higher effective gain cross-section (6.0×10^{-18} cm^2) compared with Ti:sapphire [3], which is favorable for designing laser oscillators. Ce:LiCAF has also larger saturation fluence (115 mJ/cm^2) [18] than organic dyes, which is attractive for designing power amplifiers. The fluorescence lifetime was reported to be 30 ns, which is too short for constructing regenerative amplifiers. However, it is long enough for designing multipass amplifiers. The non-polarized small-signal single-pass gain dependence on the probe beam wavelength for a 2.3-mm thick Ce:LiCAF sample with Ce^{3+} ion concentration of 0.9 at.% is shown in Fig. 1.12-(c). The sample optical axis orientation with respect to the direction of observation in this experiment was the same as for obtaining the fluorescence spectra (Fig. 1.12-(b)). The pump fluence of 0.3 J/cm^2 was used to obtain the above dependence. The probe fluence was less than 1 mJ/cm^2. From a comparison of

Fig. 1.12 (b) and (c), it is evident that the small-signal gain curve shape is similar to the fluorescence spectrum observed. This means that induced absorption is small in the gain spectral region. The small-signal gain reaches a value of 2.5 in the vicinity of the main fluorescence peak [34].

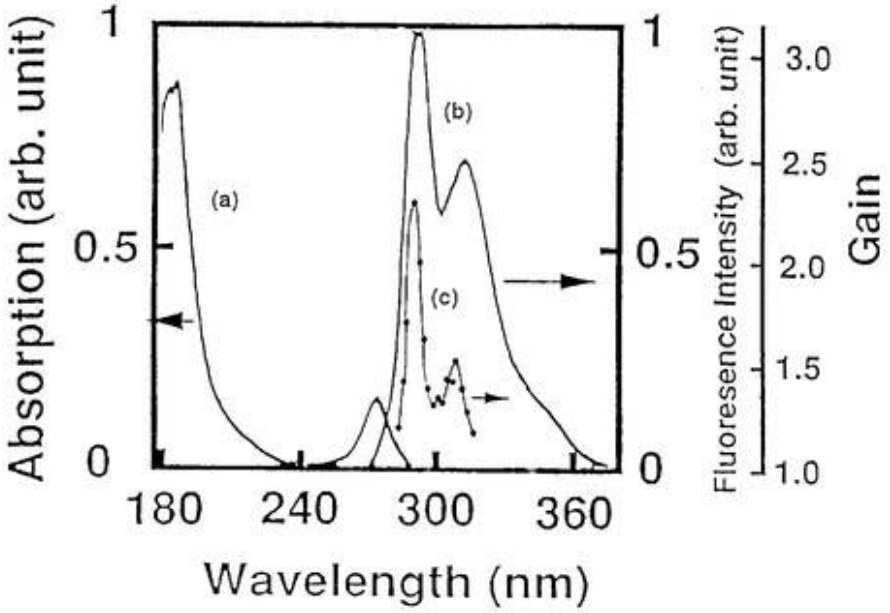

Fig. 1.12 (a) Non polarized absorption spectrum of a Ce:LiCAF sample (0.1 at. %; 2.3 mm in length); (b) Non polarized fluorescence spectrum of Ce:LiCAF (0.9 at. %); (c) Single-pass small-signal gain dependence on the probe beam wavelength for a Ce:LiCAF sample (0.9 at %; 2.3 mm in length) [34].

1.4 Purposes of this study

All these Ce-doped crystals mentioned above have broad gain-width in the ultraviolet region. Their broad gain bandwidth corresponding to a few femtoseconds is extremely attractive for short-pulse applications. In spite of their vast potential as a class of short-pulse UV laser media, there have been few short-pulse experiments done with these Ce-doped fluoride crystals.

The purpose of this study is to investigate whether the Ce:LLF and Ce:LiCAF crystals are suitable for the UV tunable short-pulse lasers or not. Here we will try to use the UV materials (1) to generate UV short pulses; (2) to

demonstrate the tunable UV laser operation; and (3) to generate high-energy UV laser pulses.

We hope our work will be useful to the people who are interested in this research field and who are finding coherent light sources in the wavelength region covered by the Ce-doped fluoride lasers.

1.5 Outline of this thesis

First the backgrounds of our research and the basic properties of Ce:LLF and Ce:LiCAF crystals are described in chapter 1.

In chapter 2, subnanosecond pulses are generated from Ce:LLF and Ce:LiCAF lasers for the first time using low-Q, short-cavity configurations. A newly-invented pumping scheme was applied to the Ce:LLF laser.

In chapter 3, the tunabilities of Ce:LLF laser and Ce:LiCAF laser are investigated. Furthermore, pulses around 230 nm are generated by sum frequency mixing of Ce:LiCAF and Nd:YAG lasers.

In chapter 4, an all-solid-state Ce:LiCAF master oscillator and power amplifier (MOPA) system is developed for demonstration of its potential for high-peak-power laser system. As a result, 289-nm, 1-ns, 14-mJ pulses were efficiently obtained from this simple laser system with 18% energy extraction efficiency in the amplifier stage.

In chapter 5, the high-energy pulses are directly generated from a Ce:LiCAF laser, due to the available large-size Ce:LiCAF crystal. The obtained pulse energy of 60 mJ is the highest output in Ce:LiCAF lasers reported until now.

In chapter 6, the author will summarize all of our contribution written in this thesis. These Ce-doped laser systems in ultraviolet region are surely premature compared with Ti:sapphire laser based systems. However, we believe such laser media including Ce:LiCAF and Ce:LLF will be utilized in

practical tunable ultraviolet ultrashort-pulse laser systems in near future. The prospect of further progress of the novel UV ultrashort pulse lasers will also be discussed.

Chapter 2. Generation of subnanosecond pulses from Ce^{3+}-doped fluoride lasers

* *J. of Nonlinear Optical Physics and Materials 8, 41-54 (1999).*

* *Applied Optics 37, 6446-6448 (1998).*

* *Applied Physics Letters 70, 3492-3494 (1997).*

Direct ultrashort pulse generation has not been obtained from ultraviolet solid-state lasers as it has for near infrared tunable laser materials like Ti:sapphire and Cr:LiSAF crystals. This is due to the difficulty of obtaining continuous-wave (CW) laser operation, which is required for Kerr lens mode-locking (KLM) schemes utilizing spatial or temporal Kerr type nonlinearity [35,36].

2.1 Short pulse generation with simple laser scheme

A general technique for subnanosecond pulse generation from laser-pumped dye laser has been described [37]. The technique makes use of the resonator transients. These transients are in the form of damped relaxation oscillation or "spiking". These resonator transients are the consequences of the interaction between the excess population inversion and the photons in the cavity. Their durations can be controlled by proper choices of photon cavity decay time and pumping level. The decay lifetime (photon lifetime) t_c of a cavity mode is defined by means of the equation:

$$\frac{dE}{dt}=-\frac{E}{t_c} \qquad (1)$$

where E is the energy stored in the mode. If the fractional (intensity) loss per pass is L and the length of the resonator is l_c, then the fractional loss per unit time is cL/nl_c, therefore

$$t_c=-\frac{nl_c}{cL} \qquad (2)$$

For the case of a resonator with mirrors' reflectivities R_1 and R_2,

$$t_c \approx \frac{nl_c}{c(1-\sqrt{R_1 R_2})} \tag{3}$$

The quality factor of the resonator is defined universally as:

$$Q=\frac{\omega E}{P}=-\frac{\omega E}{dE/dt} \tag{4}$$

where E is the stored energy, ω is the resonant frequency, and P=-dE/dt is the power dissipated. By comparing (4) and (1), we obtain

$$Q=\omega t_c \tag{5}$$

We will consider a laser resonator with two mirrors pumped by a Q-switched laser. Normally the pulse duration from the Q-switched laser is ~10 ns. During the pump pulse, inversion will build up in the laser active medium; after threshold inversion is reached, a delayed laser pulse will develop. The proposed method of short pulse generation is based on the fact that this pulse may be shorter than the pump pulse, due to the transient characteristics of the laser oscillator.

The transient behavior of such a laser can be understood by treating numerical examples with computer. The laser is adequately described by the well-known rate equations for a four-level systems as follows:

$$\frac{dn}{dt}=W(t)-Bnq \tag{6}$$

$$\frac{dq}{dt}=Bnq-\left(\frac{q}{t_c}\right) \tag{7}$$

where n is the population inversion (n_2-n_1) and nearly equal to the upper state population n_2, W(t) is the pumping rate, B is the Einstein B coefficient for stimulated emission, q is the total number of photons in the cavity, t_c is the resonator (photon) lifetime.

The pumping rate was assumed to have the form of a Gaussian pulse with full half-width T_1 and integrated photon number N. A large reduction of the over-all pulse duration demands a high value of T_1/t_c. The ratio T_1/t_c can be made large easily, since the laser resonator needs no switching elements and therefore need not be longer than the material itself. Further, it is possible to use a laser resonator of low mirror reflectivity, whose resonator lifetime is not markedly longer than the single-pass transit time l_c/c. To obtain short single pulses, it is necessary to use resonator lifetimes which are small compared to the pump duration in combination with controlling the level of pumping [38].

2.2 Subnanosecond Ce:LLF laser pumped by the fifth harmonic of Nd:YAG laser [39]

Figure 2.1 indicates the absorption spectrum (nonpolarized) of a Ce:LLF sample containing 1 atomic % of Ce^{3+} ions (in the melt). Considering the Ce:LLF absorption, one can see that while this material does not noticeably absorb at 266 nm, it will absorb pumping radiation at the fifth harmonic of Nd:YAG laser wavelength (213 nm) almost as efficiently as at the KrF-excimer pumping wavelength of 248 nm. With the recent development of new nonlinear borate crystal materials such as $CsLiB_6O_{10}$ [40] and $Li_2B_4O_7$ [41], the fifth harmonic of Nd:YAG lasers has become usable and practical due to the significantly improved efficiency and stability, close to those typical of the fourth harmonic of Nd:YAG laser. Hence, direct pumping of tunable laser medium Ce:LLF by the fifth harmonic of conventional Nd:YAG lasers has become practical.

From Fig. 2.1, it is evident that even the off-peak absorption at 213 nm is strong enough to consider the crystal suitable for an all-solid-state approach using the fifth harmonic of an Nd:YAG laser for side pumping. To prove this, we tested the Ce:LLF under side pumping conditions by the fifth harmonic of an

Nd:YAG laser. The 213-nm, 25-mJ, 5-ns, horizontally polarized pulses (σ-pumping) for pumping Ce:LLF laser were stably obtained in $Li_2B_4O_7$ crystal using the type-I sum frequency generation process between 1064-nm and 266-nm pulses from a conventional Q-switched Nd:YAG laser [41]. The optical layout for a short-cavity Ce:LLF laser is shown schematically in Fig. 2.2.

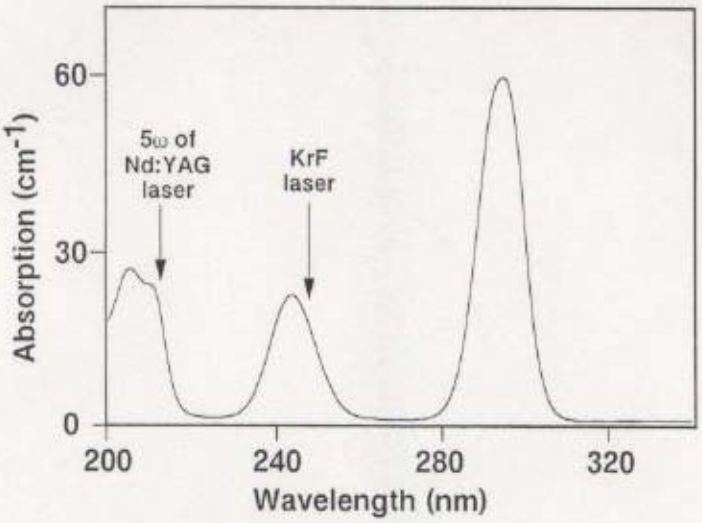

Fig. 2.1 Nonpolarized absorption spectrum of Ce^{3+} ions in $LiLuF_4$ single crystal (Cerium concentration in melt - 1 atomic %).

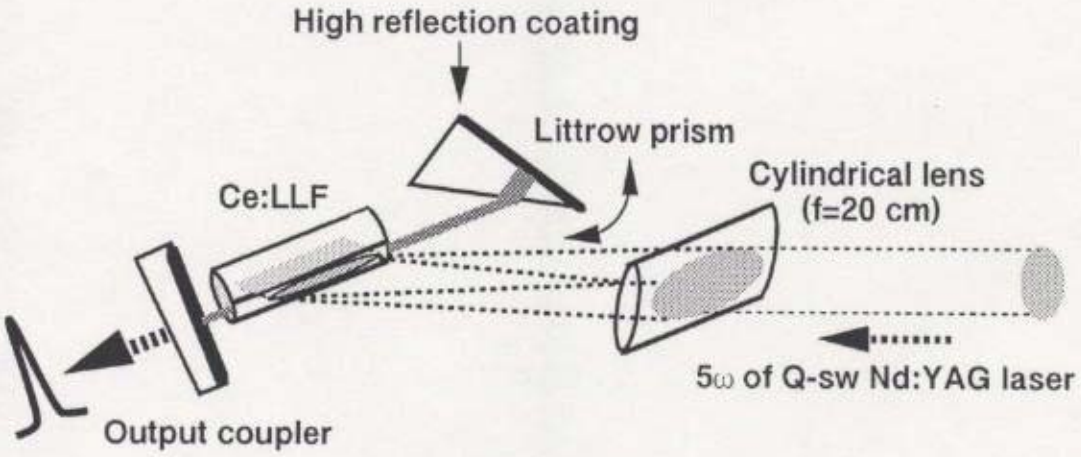

Fig. 2.2 Short-cavity, tilted-incidence-angle (approximately 70 degrees) side pumping tunable Ce:LLF laser optical layout. The pumping pulse was focused by a 20-cm focal length cylindrical lens tilted so that the cylinder axis is parallel to the side window of the laser crystal.

The Ce:LLF single crystal with 0.2 atomic % doping level was cut to form a cylinder (5-mm diameter and 25-mm length) with a flat polished window on the side. The sample was oriented so that its optical axis was parallel to the side window and perpendicular to the cylinder longitudinal axis. No antireflection coatings were applied to the rod ends for this experiment. To increase the efficiency of side pumping, we geometrically reduced the effective pumping penetration depth using the novel tilted-incidence-angle side pumping scheme instead of conventional normal-incidence side pumping. Using a 20-cm-focal-length cylindrical lens which was also tilted to be parallel to the side window of the laser crystal, the pumping pulse was focused down to a 1.2 x 0.15 cm^2 line-shaped area to provide the 140 mJ/cm^2 pumping fluence at nearly 70-degree incidence angle. Observed efficient penetration depth was estimated to be ~1 mm, meanwhile in conventional normal-incidence side pumping scheme, the pumping penetration depth was over 3-mm for the Ce:LLF crystal used here, which is too deep for obtaining a good output beam pattern. Obvious advantages of the above-mentioned tilted-incidence-angle, side-pumping scheme are very simple focusing geometry, reduced pumping fluence at the rod surface, reduced risk of damaging optics, and better matching of the excited rod volume and the laser cavity mode volumes (quite similar to the coaxial pumping scheme). This better matching resulted in a better output beam quality. The low-Q, short-cavity Ce:LLF laser consisted of a Littrow prism which was used as an end mirror, and a low reflection (20%) flat output coupler. The total length of the laser cavity was 6 cm. Typical spectrally and temporally resolved streak-camera images of the Ce:LLF laser output pulse are given in Fig. 2.3. Using the 213-nm, 5-ns, 16-mJ pumping pulses, we were able to obtain 880-ps, 77-μJ, σ-polarized, and satellite-free reproducible pulses at 309 nm. It is worth mentioning here that pumping at 213 nm does not cause noticeable laser rod

solarization or laser performance degradation during several hours of continuous operation at a 10-Hz repetition rate.

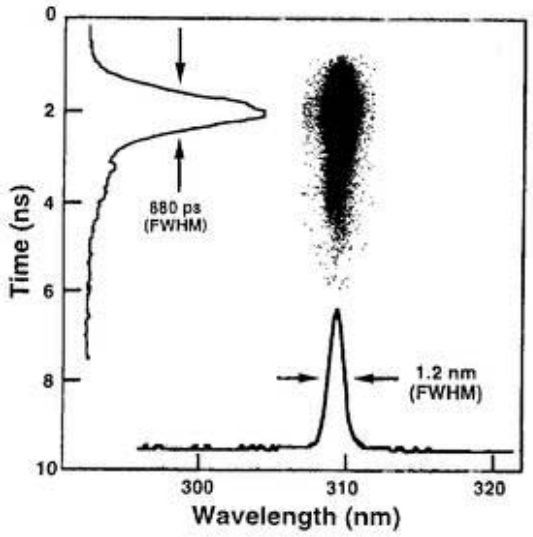

Fig. 2.3 Temporally and spectrally resolved streak-camera image of UV short pulse from a low-Q, short-cavity Ce:LLF laser.

2.3 Short pulse generation from Ce:LiCAF laser

2.3.1 Short pulse generation from Ce:LiCAF laser with nanosecond pumping

Ce:LiCAF is a tunable UV laser medium which can be directly pumped by the fourth harmonic of a standard Nd:YAG laser. A 1% doped, 5-mm cubic Ce:LiCAF sample was used without any dielectric coatings on the polished surfaces. The experimental setup of the subnanosecond Ce:LiCAF laser is shown in Fig. 2.4. The 1.5-cm long laser cavity was formed by a flat high-reflection mirror and an 80% transmission flat output coupler. 20-mJ, 10-ns, 1-Hz, 266-nm, horizontally polarized pumping pulses (the fourth harmonic of a conventional 10-ns Q-switched Nd:YAG laser) were focused longitudinally from the high-reflection mirror side by a 30-cm focal-length lens with ~300 mJ/cm^2 pumping fluence inside the active medium. The c-axis of the Ce:LiCAF

laser crystal sample was parallel to the direction of the pumping polarization. The absorbed energy was 5 mJ. The single output pulse has a energy of 45 μJ. The pulse duration was measured to be 600 ps using a streak camera. In this simple way, we can generate subnanosecond pulse from an all-solid-state Ce:LiCAF laser pumped by a 10-ns Q-sw Nd:YAG laser.

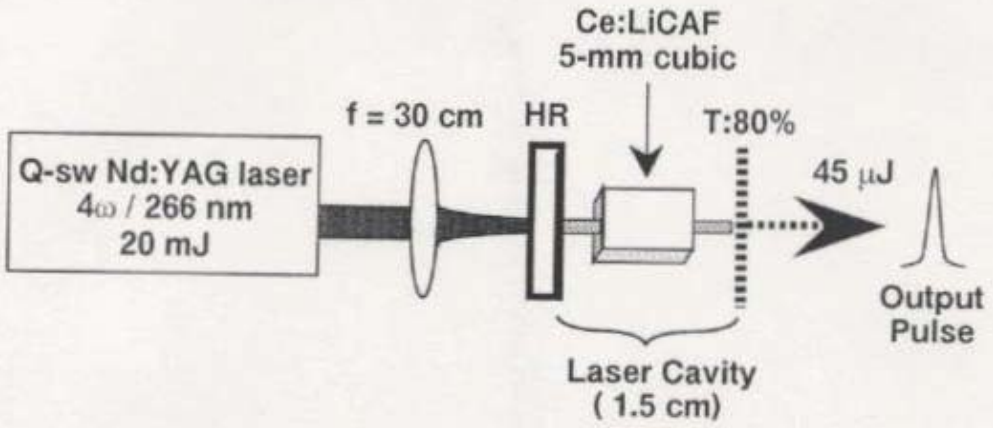

Fig. 2.4 Experimental setup of low-Q, short-cavity Ce:LiCAF oscillator with nanosecond pumping.

2.3.2 Short pulse generation from Ce:LiCAF laser with picosecond pumping [42]

We have generated 600-ps pulses from a low-Q, short-cavity Ce:LiCAF laser pumped by the fourth-harmonic of a Q-sw 10-ns Nd:YAG laser above. For shorter pulse generation we tried to use a shorter pumping source: the fourth harmonic of a mode-locked Nd:YAG oscillator and regenerative amplifier system operated with the repetition rate of 10 Hz. A low-Q, short cavity Ce:LiCAF oscillator was formed by a flat high-reflection mirror and a 30% reflection flat output coupler. The cavity length was 1.5 cm. A 10-mm Brewster-cut, 1% doped (in the melt) Ce:LiCAF crystal was used. A typical spectrally and temporally resolved streak camera image of the output pulse of the Ce:LiCAF laser is shown in Fig. 2.5. The Ce:LiCAF laser pulse width was measured to be 150 ps, while the pumping pulse width was 75 ps.

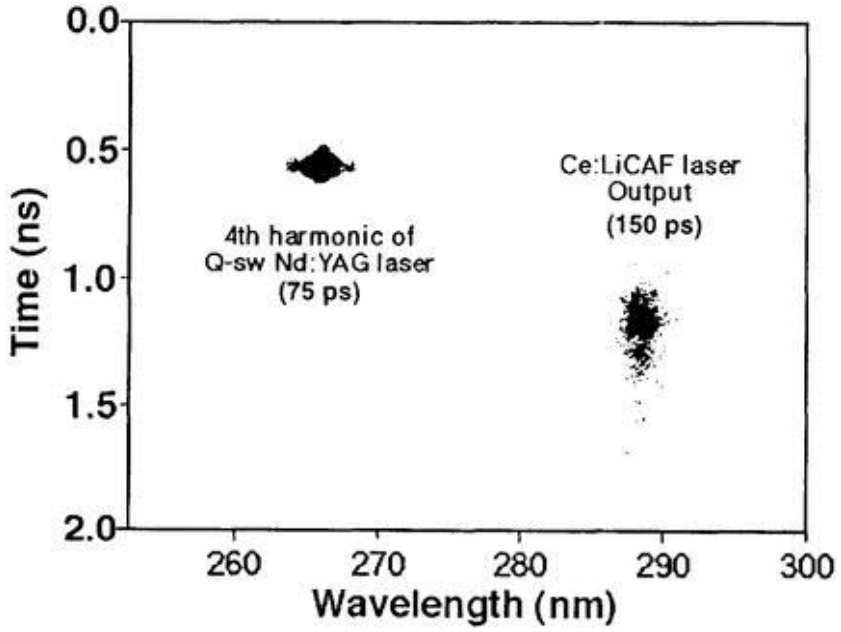

Fig. 2.5 Streak camera image of the low-Q, short-cavity Ce:LiCAF laser pulse with picosecond pumping.

Summary: We demonstrated that the sub-nanosecond pulses can be generated simply from low-Q, short-cavity Ce:LLF laser pumped by the fifth harmonic of 10-ns Q-switched Nd:YAG laser, and Ce:LiCAF laser pumped by the fourth harmonics of 10-ns Q-switched Nd:YAG laser or picosecond mode-locked Nd:YAG laser.

Chapter 3. Ultraviolet tunable pulse generation from Ce^{3+}-doped fluoride lasers

* *J. of Nonlinear Optical Physics and Materials* **8**, 41-54 (1999).

* *Applied Optics* **37**, 6446-6448 (1998).

* *Japanese J. of Applied Physics* **37**, L36-L38 (1998).

* *Japanese J. of Applied Physics* **36**, L1384-L1386 (1997).

In most lasers, all of the energy released via stimulated emission by the excited medium is in the form of photons. Tunability of the emission in solid-state lasers is achieved when the stimulated emission of photons is intimately coupled to the emission of vibrational quanta (phonons) in a crystal lattice. In these "vibronic" lasers, the total energy of the lasing transition is fixed, but can be partitioned between photons and phonons in a continuous fashion. The result is broad wavelength tunability of the laser output. In other words, the existence of tunable solid-state lasers is due to the subtle interplay between the Coulomb field of the lasing ion, the crystal field of the host lattice, and electron-phonon coupling permitting broad-band absorption and emission. Therefore, the gain in vibronic lasers depends on transitions between coupled vibrational and electronic states; that is, a phonon is either emitted or absorbed with each electronic transition.

Rare earth ions doped in appropriate host crystals exhibit vibronic lasing. The main difference between transition metal and rare earth ions is that the former is crystal field sensitive and the latter is not. As distinct from transition metal ions, the broad-band transition for rare earth ions are quantum mechanically allowed and therefore have short lifetime and high cross-sections. The Ce^{3+} ion laser, using a 5d-4f transition, has operated in the host crystals. Such a system would be alternative to the excimer laser as a UV source, with the added advantage of broad tunability.

Due to the vibronic nature of the Ce^{3+} ion laser, the emission of a photon is accompanied by the emission of phonons. These phonons contribute to thermalization of the ground-state vibrational levels. The laser wavelength depends on which vibrationally excited terminal level acts as the transition terminus; any energy not released by the laser photon will then be carried off by a vibrational phonon, leaving the Ce^{3+} ion at its ground state. The terminal laser level is a set of vibrational states well above the ground state. So the Ce^{3+} ion lasers belong to 4-level lasers.

3.1 Tunable Ce:LLF laser [39]

The fluorescence spectrum of Ce:LLF crystal excited by the fifth harmonic of an Nd:YAG laser is shown in Fig. 3.1. The Ce:LLF crystal was the one used in the experiment of Sec. 2.2. There are two peaks around 308 nm and 325 nm seen

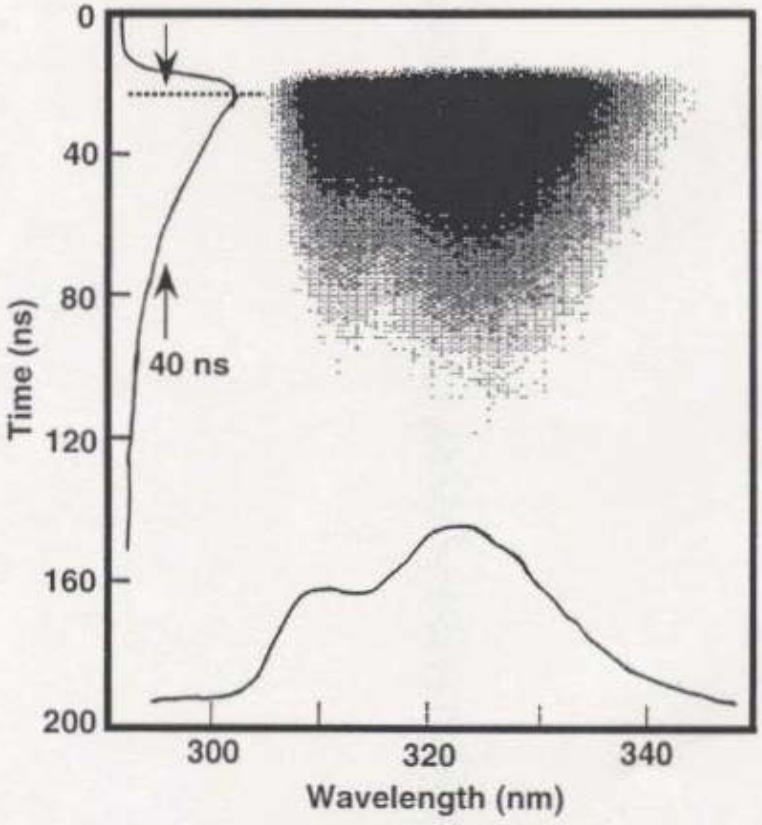

Fig. 3.1 Spectrum of Ce:LLF pumped by the fifth harmonic of an Nd:YAG laser. There are two peaks around 308 nm and 325 nm. The fluorescence lifetime is 40 ns.

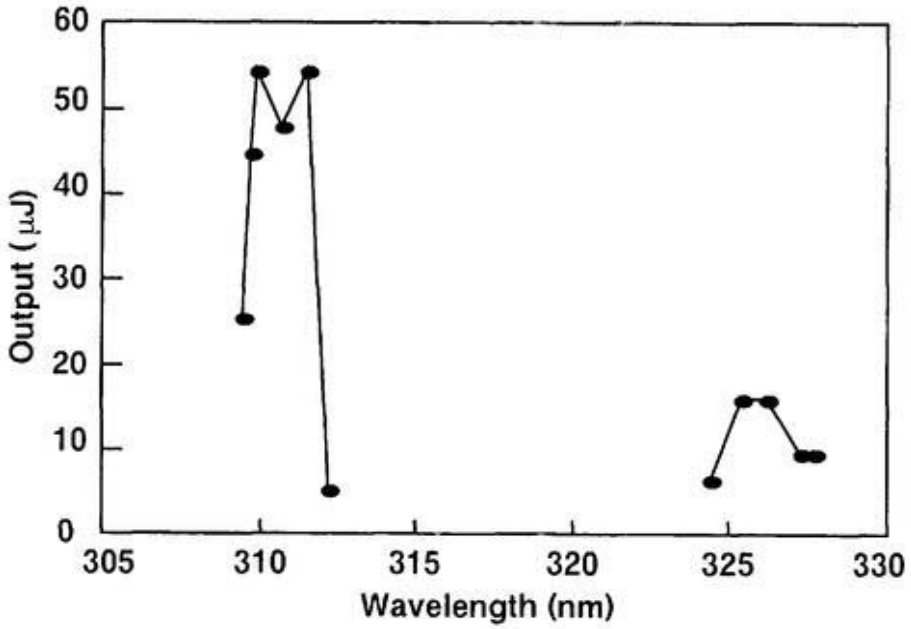

Fig. 3.2 Short-cavity, high-Q Ce:LLF laser tunability obtained at a pumping energy of 22 mJ at 213 nm.

from the fluorescence spectrum. The fluorescence life time of the Ce:LLF crystal was estimated to be 40 ns. To test the Ce:LLF laser tunability under 213-nm pumping conditions, we employed a high-Q cavity by replacing the output coupler shown in Fig. 2.2 with an 80% reflection flat mirror. Tunable operation was realized by rotating the prism about the vertical axis. The Ce:LLF laser tunability obtained at the pumping energy level of 22 mJ at 213 nm is shown in Fig. 3.2. In a subnanosecond-pulse regime, the tuning was achieved from 309.5 nm to 312.3 nm and from 324.5 nm to 327.7 nm. The gap in the tuning curve is attributed to the close-to-the-threshold operation regime necessary to maintain a single subnanosecond pulse operation. This tuning behavior resembles the one for Ce:YLF laser [43].

3.2. Tunable Ce:LiCAF laser [44,45]

The experimental setup of the tunable short-cavity Ce:LiCAF laser is shown schematically in Fig. 3.3. The cavity length was 25 mm. To study the

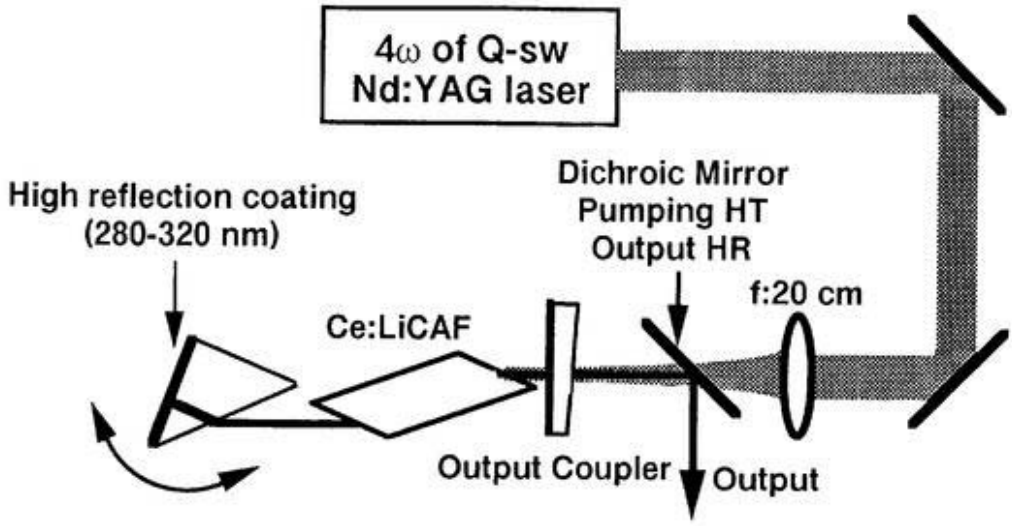

Fig. 3.3 Experimental setup of the tunable, short-cavity Ce:LiCAF oscillator pumped by the fourth harmonics of a Q-switched Nd:YAG laser.

tuning performance of this laser without consideration of its temporal characteristics, we designed a high-Q laser with a low transmission flat output coupler (T=20%). The laser consisted of a half-cut Brewster prism with a high reflection coating at one face used as the end mirror and a 10-mm-long Brewster-cut at the end faces 1% doped (in the melt) Ce:LiCAF crystal used as the gain medium without any special cooling. The 266-nm, horizontally polarized pumping pulses from a Q-switched Nd:YAG laser in short-pulse operation mode were focused longitudinally from the output mirror side using a 20-cm-focal-length lens. In a single pumping shot, there were 4 short pulses with pulse durations of about 1 ns separated by about 5 ns as shown in Figs. 3.6 and 3.7. In most cases, the laser operated at 2 Hz to reduce any possible thermal problems in the Ce:LiCAF crystal without mandatory cooling, and to obtain higher extraction efficiency. The c-axis of the Ce:LiCAF crystal was parallel to the direction of the pumping polarization. The tuning operation was realized by rotating the prism horizontally. Tuning using a Ce:LiCAF crystal with Brewster-cut end faces is very efficient because it can increase the dispersion of

the laser beam. The output pulse was separated from the pumping beam by a dichroic mirror which has high reflection in the region of 280-320 nm at a 45-degree incidence angle and high transmission for the pumping beam (266 nm). The output pulse energy tuning curve obtained is shown in Fig. 3.4 with the pumping energy of 8 mJ. As illustrated in Fig. 3.4, the pulses were multi-peak at some points in the form of damped relaxation oscillation, and the main peaks had pulse durations of 2 to 3 nanoseconds. The corresponding tuning was accomplished from 282 nm to 314 nm, sacrificing the capability of single-short-pulse generation.

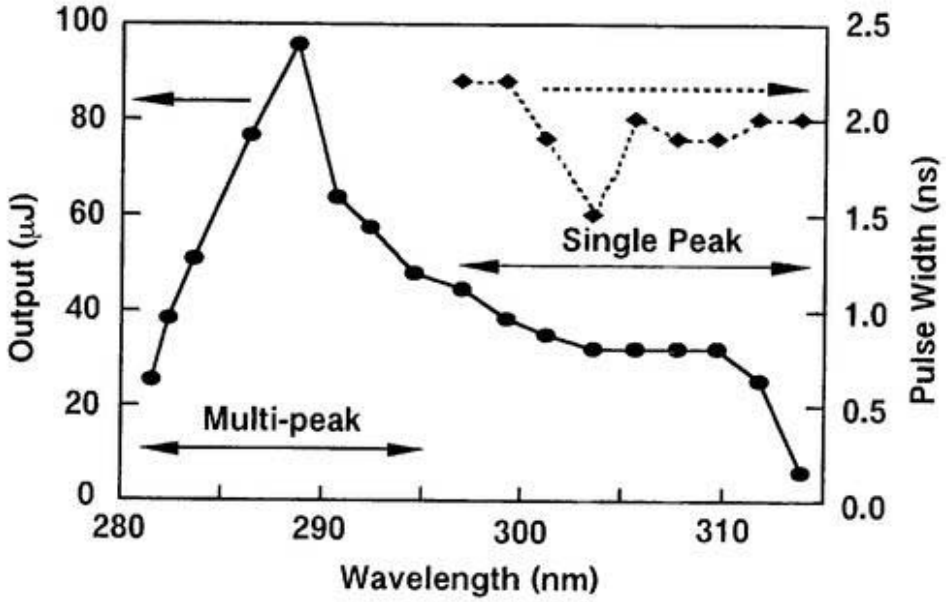

Fig. 3.4 For the high-Q (T_C=20%), short cavity Ce:LiCAF laser, tunability between 282 and 314 nm was obtained.

To obtain shorter pulses and a single-pulse output, we constructed a low-Q, short-cavity Ce:LiCAF laser by changing the output coupler of the laser mentioned above to a 75% transmission flat coupler. The output pulse energy dependence on wavelength is shown in Fig. 3.5. The pumping energies for different wavelengths were varied between 2 to 4 mJ to obtain single-pulse generation. The demonstrated tuning range was 281 nm to 297 nm. The pulse

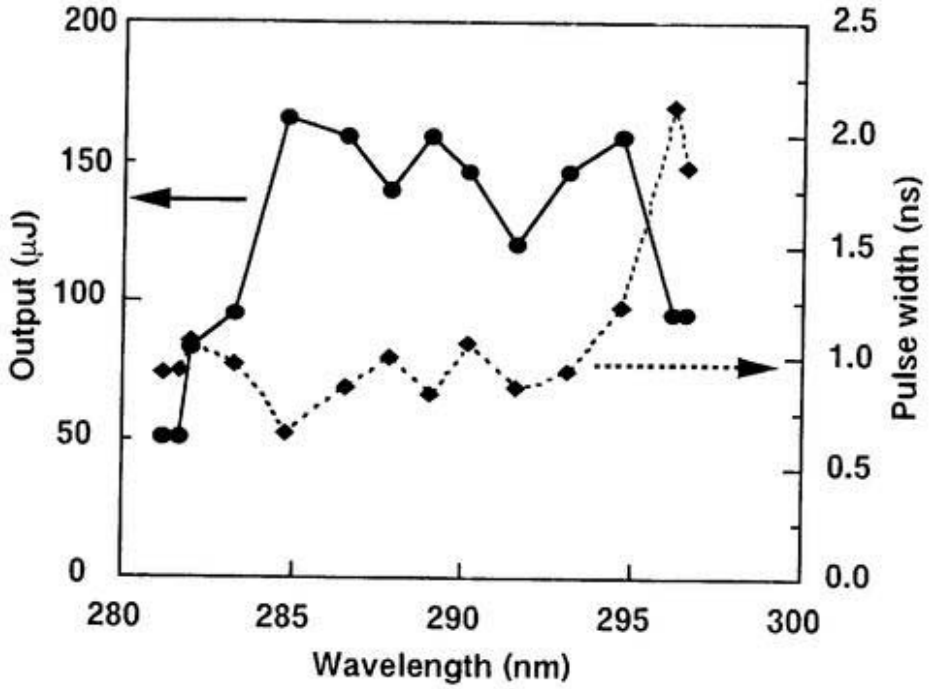

Fig. 3.5 From the low-Q (T_C=75%), short cavity Ce:LiCAF laser with a tuning-prism-type end mirror, tunability from 281 to 297 nm was achieved while maintaining single short pulse properties.

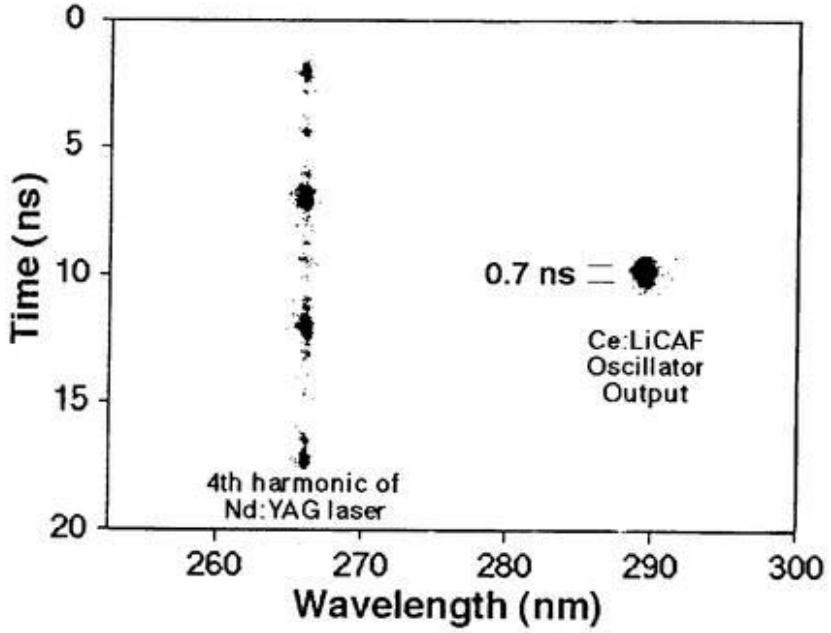

Fig. 3.6 Spectrally and temporally resolved streak camera image of the output pulse at 289 nm from the low-Q, short-cavity Ce:LiCAF laser. The image of the pumping pulse can also be observed.

durations at different wavelengths observed by a streak camera are also shown in Fig. 3.5. Under the appropriate pumping fluence control, no satellite pulse was observed because the pulse duration exceeded the cavity round trip time (170 ps). The typical spectrally and temporally resolved streak camera image of the output pulse at a wavelength of 289 nm including the image of the pumping pulse is given in Fig. 3.6. They were taken in a single shot. Figure 3.7 was derived from Fig. 3.6 and describes the temporally resolved streak camera traces of the output pulse and the pumping pulse [53].

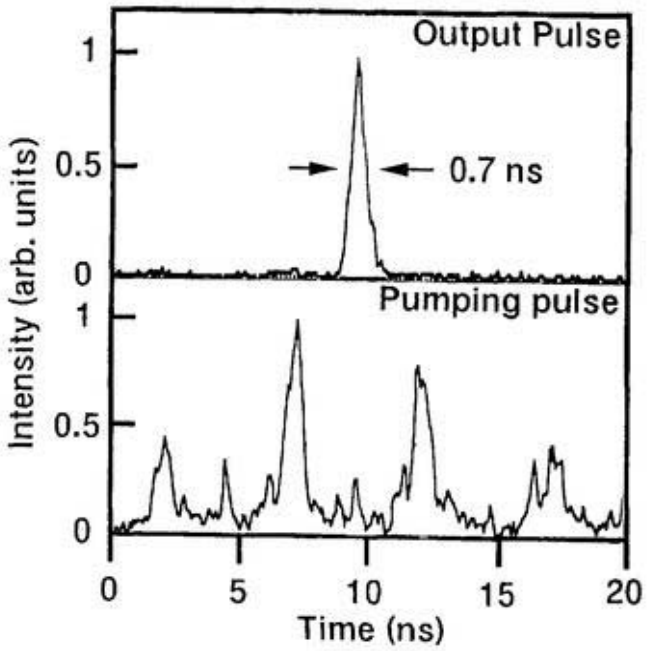

Fig. 3.7 Temporally resolved streak camera traces of the output pulse and the pumping pulse processed from the image in Fig. 3.6. The pulse width (at half maximum) of the output pulse was 0.7 ns, and the center wavelength was 289 nm with a spectrum width (at half maximum) of about 2 nm.

To increase the output energy while maintain the single short output pulse, a 55% reflection flat output coupler was used. A single-pulse output was generated with the pumping energy of 15 mJ. The demonstrated tuning range was 282 nm to 314 nm (Fig. 3.8). The maximum single subnanosecond pulse output was 1 mJ with the pulse width of 0.9 ns observed by a streak camera. In

this way, single short pulses with broad tuning regions can be easily generated from a low-Q, short-cavity, tunable Ce:LiCAF laser pumped by the fourth harmonic of a Q-switched Nd:YAG laser.

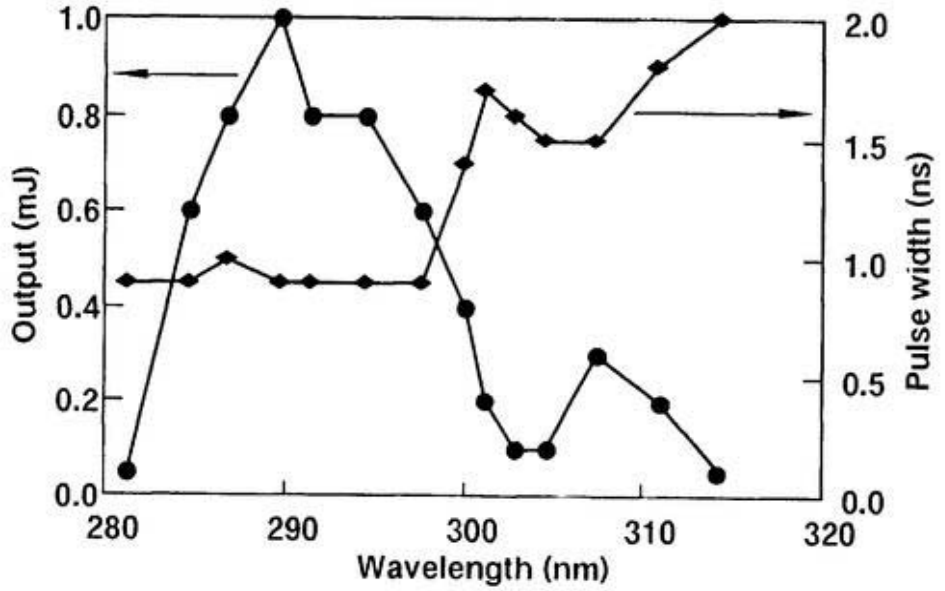

Fig. 3.8 Tuning curve for the short-cavity Ce:LiCAF laser with 55% reflection output coupler.

3.3. Tunable pulse generation around 230 nm by sum-frequency mixing [45]

To obtain tunable short UV pulses around 230 nm, short pulses from a tunable Ce:LiCAF MOPA system were mixed with the fundamental radiation of a Q-switched Nd:YAG laser. The spectral region covered by this sum frequency generation lies between the fourth and fifth harmonics of Nd lasers and also between the third and fourth harmonics of tunable near-infrared lasers such as Cr:LiSAF. The spectral region near 230 nm is practically important because it spans the signature absorption features of chemical and biological species such as nitric oxide, and tryptophan.

The experimental setup is shown schematically in Fig. 3.9. The oscillator stage of the MOPA system is the same as mentioned above (see Sec. 3.2). The

double-side-pumping, double-pass-amplification configuration was applied in the amplifier stage. A Q-switched Nd:YAG laser was used to pump the oscillator and amplifier stages with optimized optical delay. 266-nm pulses with 12-mJ and 15-mJ energies from each side were slightly focused on the Ce:LiCAF crystal of the amplifier. We adjusted the pump energy for the Ce:LiCAF oscillator to obtain a better beam pattern so that we could increase the efficiency of the amplifier. An energy tuning curve for the Ce:LiCAF MOPA system is shown in Fig. 3.10. Continuous tunability of the MOPA system was obtained from 284 nm to 299 nm with the maximum pulse energy up to 4 mJ.

A BBO nonlinear crystal is utilized for frequency mixing of the Ce:LiCAF MOPA system output with the fundamental output of another Q-sw Nd:YAG

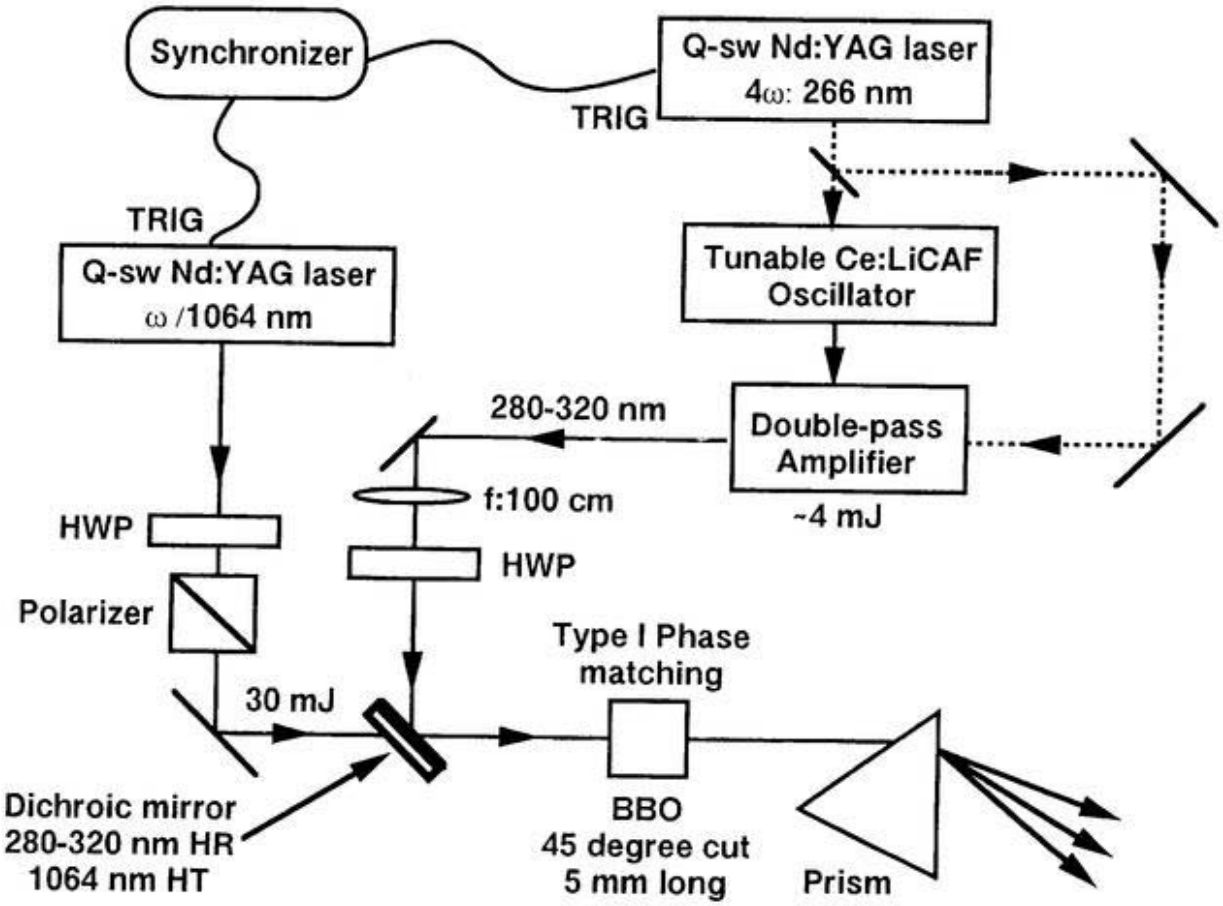

Fig. 3.9 Experimental setup of sum-frequency mixing of Ce:LiCAF and Nd:YAG laser beams through a BBO crystal in Type-I phase matching condition.

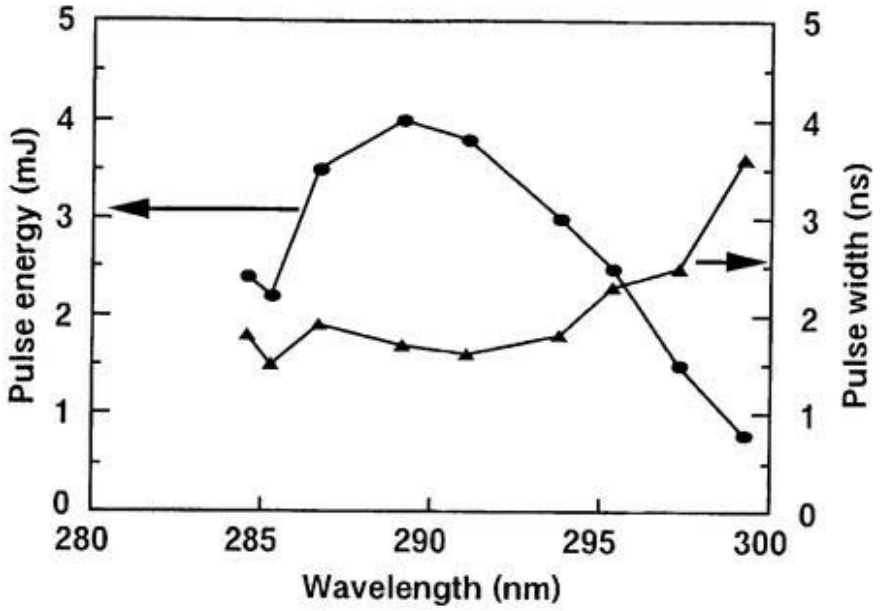

Fig. 3.10 Tuning curve for the Ce:LiCAF MOPA system for the sum frequency mixing with Nd:YAG laser.

laser which is synchronized to the Nd:YAG laser for pumping the Ce:LiCAF MOPA system. The BBO crystal (5 mm x 5 mm x 5 mm) is cut at θ=45 degree for Type-I phase-matching. The Ce:LiCAF laser beam was focused with a 100-cm-focal-length lens. Using a dichroic beam splitter, the Ce:LiCAF and Nd:YAG laser beams were spatially overlapped and subsequently input into the BBO crystal. The delay between the Ce:LiCAF and Nd:YAG laser beams was electrically controlled to ensure temporal overlapping of the two input beams. Pulse energy of the Nd:YAG laser fundamental beam was 30 mJ. The tunability after the sum-frequency-mixing is shown in Fig. 3.11. Obtained tuning region was from 223 nm to 232 nm. Sum-frequency generation was optimized at each wavelength by angle tuning the BBO crystal to maintain the proper phase-matching. The peak of the tuning occurred at 227 nm with 0.5 mJ of output energy. The spectrally and temporally resolved streak camera image of the output pulse at this wavelength is given in Fig. 3.12, and the pulse width was measured to be 1.0 ns.

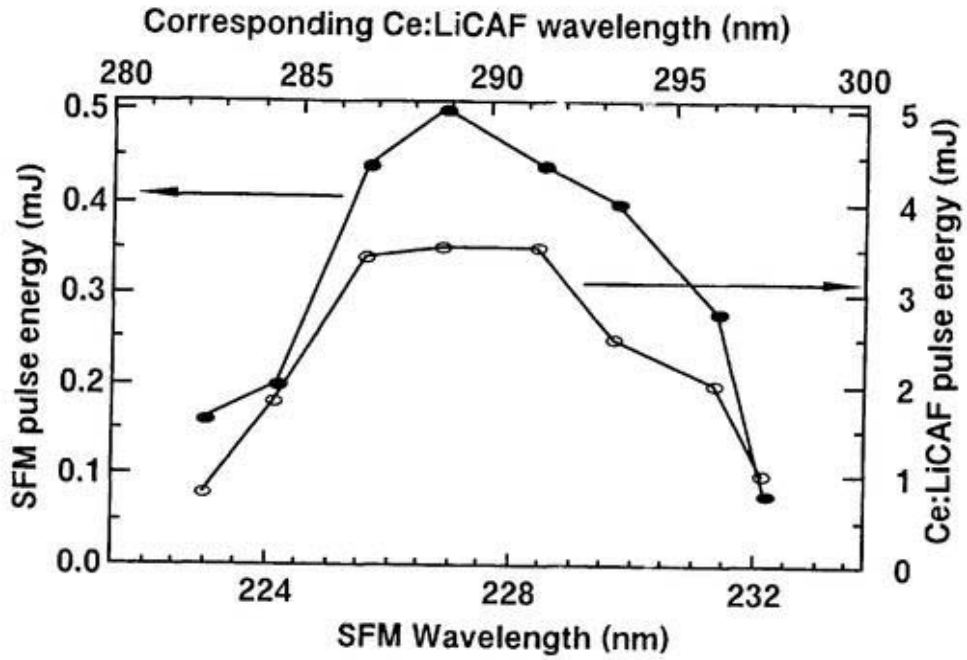

Fig. 3.11 Tuning curve for sum-frequency mixing of Ce:LiCAF and Nd:YAG laser beams.

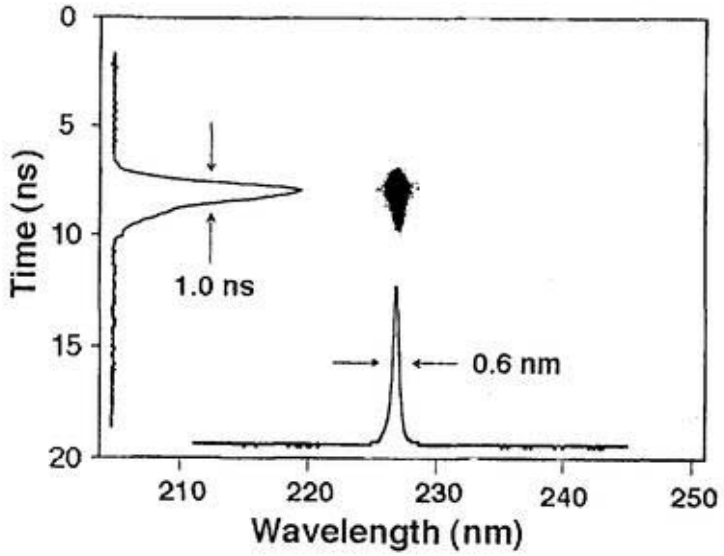

Fig. 3.12 Spectrally and temporally resolved streak camera image of the sum-frequency generation at the peak point of the tuning curve of Fig. 3.11.

Summary: The tunability of Ce:LLF laser was investigated using a newly-invented tilted-incidence-angle pumping scheme with the fifth harmonic of Q-switched Nd:YAG laser as the pumping source. The tunable Ce:LiCAF laser generated output pulses from 282 nm to 314 nm. Furthermore, pulses from 223 nm to 232 nm were generated by the sum-frequency mixing of a tunable Ce:LiCAF MOPA system and the fundamental of a Q-switched Nd:YAG laser.

Chapter 4. Efficient UV short-pulse amplification in a Ce:LiCAF MOPA system [46]

* *J. of Nonlinear Optical Physics and Materials 8, 41-54 (1999).*

* *Optics Letters 22, 994-996 (1997).*

The generation of high-energy pulses is based on the combination of a master oscillator and multistage power amplifiers. In a oscillator-amplifier system, pulse width, beam divergence, and spectral width are primarily determined by the oscillator, whereas pulse energy and power are determined by the amplifier. Operating an oscillator at relatively low energy levels reduces beam divergence and spectral width. Therefore, from an oscillator-amplifier combination one can obtain either a higher energy than is achievable from an oscillator alone or the same energy in a beam which has a smaller beam divergence and narrower linewidth. Generally speaking, the purpose of adding an amplifier to a laser oscillator is to increase the brightness B [W cm^{-2} sr^{-1}] of the output beam

$$B=P/A\Omega$$

where P is the power of the output beam emitted from the area A, and Ω is the solid-angle divergence of the beam.

The experiment setup of a Ce:LiCAF MOPA system is shown in Fig. 4.1. A low-Q, short cavity Ce:LiCAF master oscillator with 15-mm cavity length was formed by a flat high-reflection mirror and a 30% reflection flat output coupler. A 10-mm Brewster-cut, 1% doped (in the melt) Ce:LiCAF crystal was used as the oscillator gain medium. 15-mJ, 10-ns, 266-nm, horizontally polarized pumping pulses from a Q-switched Nd:YAG laser were focused longitudinally from the high-reflection mirror side by a 20-cm focal-length lens to obtain a 1 J/cm^2 pumping fluence inside the active medium. In most cases, the laser operated at 2 Hz to avoid possible thermal problems in the Ce:LiCAF crystal

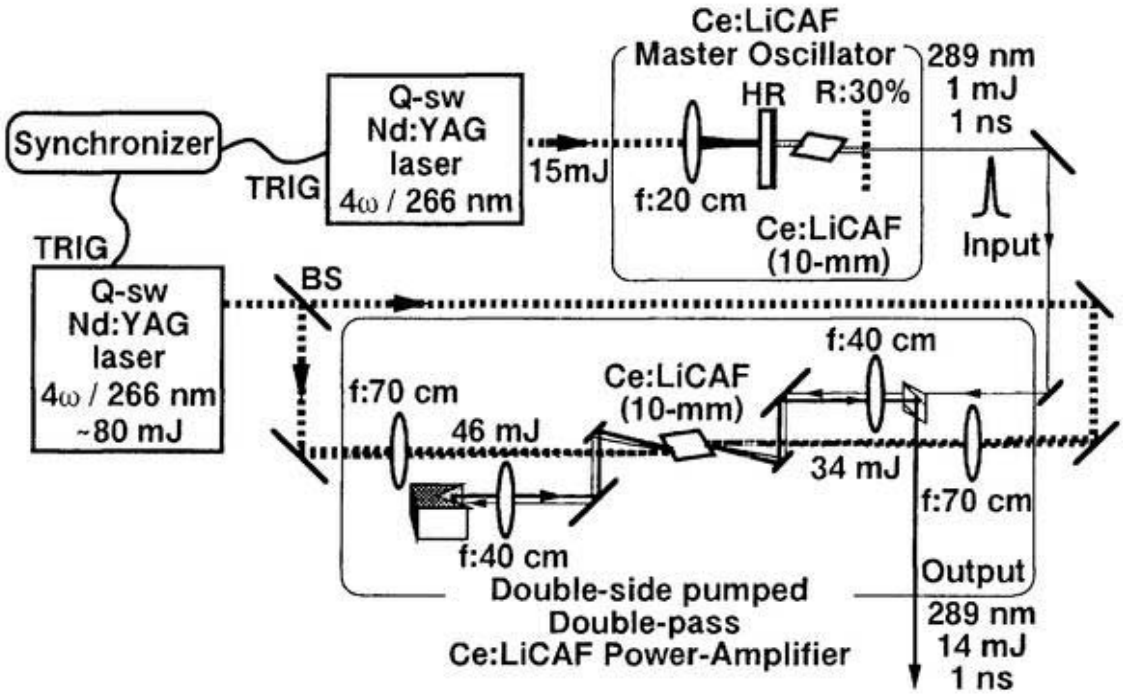

Fig. 4.1 Experiment setup of the Ce:LiCAF MOPA system pumped by fourth harmonics of two conventional 10-ns Q-switched Nd:YAG lasers. This system consists of a low-Q, short-cavity master oscillator, and a confocal double-pass power amplifier.

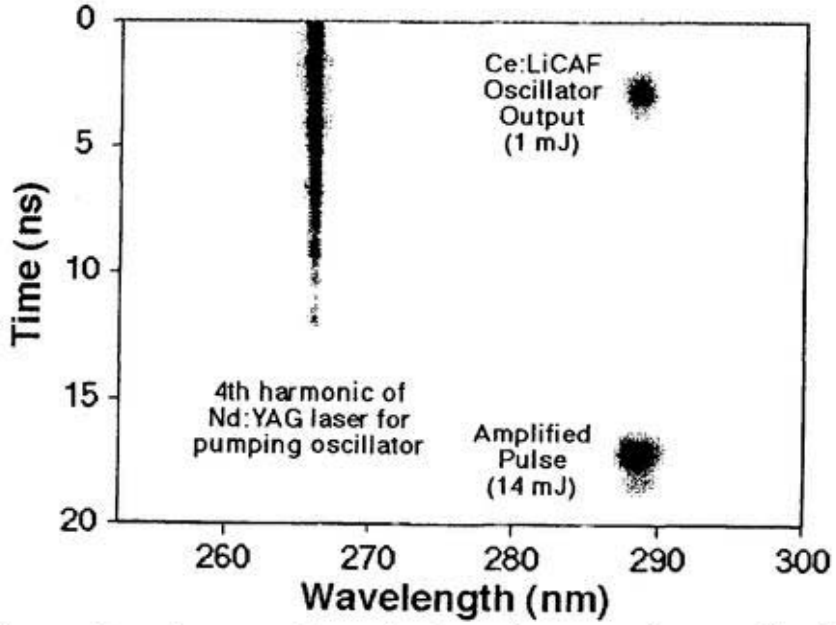

Fig. 4.2 Spectrally and temporally resolved streak-camera image of the UV short pulses from the oscillator stage and after the amplifier stage. A part of the oscillator-pumping pulse image can also be observed. All these images are taken in a single shot.

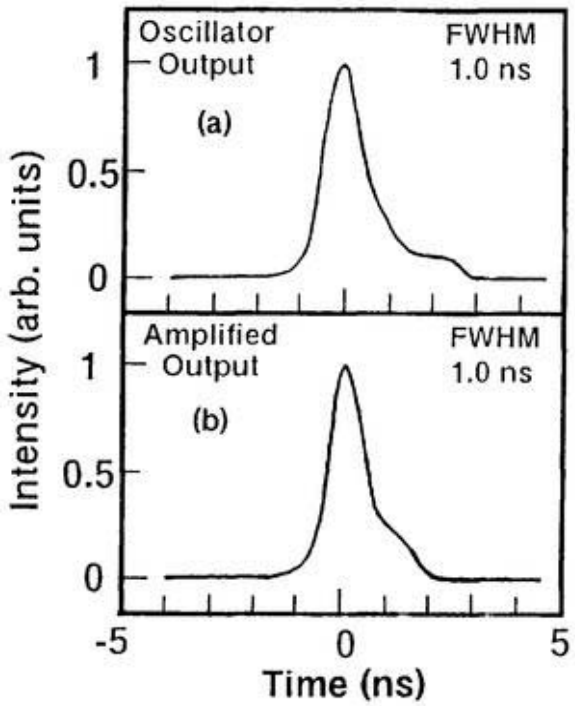

Fig. 4.3 Temporally resolved streak-camera traces of the pulses processed from the image in Fig. 4.2. (a) The temporal pulse shape from the low-Q, short-cavity master oscillator. The pulse duration (FWHM) was 1.0 ns, and the center wavelength was 289 nm. (b) The temporal pulse shape after the amplifier. The pulse duration (FWHM) was also 1.0 ns.

and to obtain higher extraction efficiency. The c-axis of the Ce:LiCAF crystal was parallel to the direction of the pumping polarization. A single 1-mJ, horizontally polarized pulse at 289-nm was obtained at the sacrifice of the extracted energy from this master oscillator. The pulse duration observed by a streak camera was 1.0-ns as shown in Fig. 4.2 and Fig. 4.3(a). Under the appropriate pumping fluence control, no satellite pulse was observed because the pulse duration exceeded the cavity round trip time (100 ps).

Another 10-mm, 1%-doped Brewster-cut Ce:LiCAF crystal was employed in the power amplifier stage. The amplifier was designed with a confocal double-pass configuration similar to the double-sided, coaxially-pumped, confocal-multipass configuration of a Ti:sapphire amplifier [47]. Another 10-ns, Q-switched Nd:YAG laser for pumping the amplifier operated

with variable Q-switch delay. 266-nm pulses with 46-mJ and 34-mJ energies from each side were slightly focused by 70-cm focal-length lens down to ~1-mm beam diameter (~ 5 J/cm^2). The amplifier consisted of a gain medium located at the beam waist of a confocal lens pair (40-cm focal-length) and a roof-reflector with dielectric coating for a small vertical displacement of each pass (Fig. 4.1). The signal passes coincide with the pumped region with a small angular separation from the pumping beams (less than a few degrees). This configuration allowed the signal beams with different passes to overlap almost completely in a small pumped region. The output energy of the amplifier was measured for different pumping delays as shown in Fig. 4.4. This result indicates that the relative timing between two Nd:YAG lasers should be controlled within an accuracy of a few nanoseconds. Here the optimum relative delay timing between the Q-switch trigger signals for the two Nd:YAG lasers was 15 ns. A single-pass gain of over 10 times was observed. The double-pass differential small-signal gain reaches 100 times as shown in Fig. 4.5. The 1-mJ

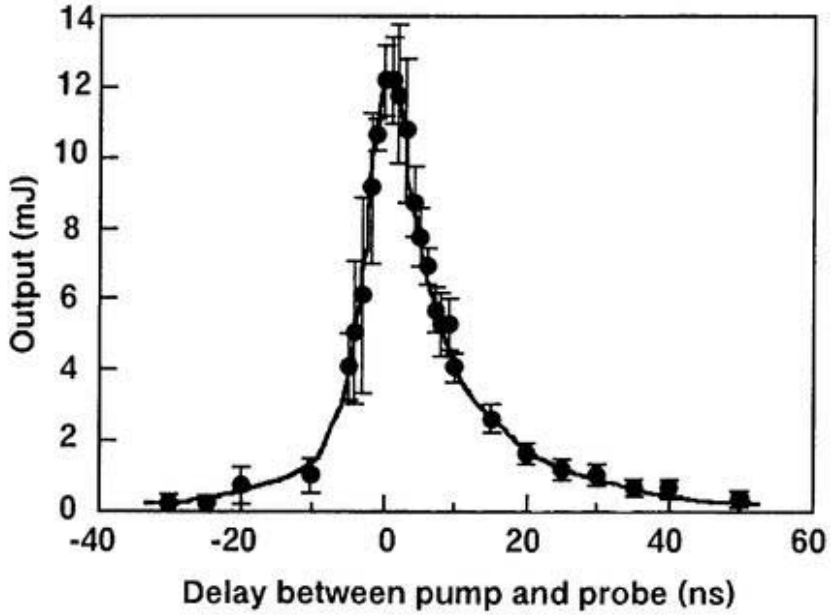

Fig. 4.4 Output energy of the amplifier for different delay timings of the probe pulse from the oscillator and the amplifier-pumping pulse from the Nd:YAG laser.

input pulse was amplified up to 14-mJ with 14-MW peak power at a 2-Hz repetition rate. The amplified pulse duration observed by a streak camera was 1.0-ns as shown in Fig. 4.3(b). There was no noticeable pulse broadening accompanying the amplification process. The output gain dependence on different input energy of the amplifier is shown in Fig. 4.5. This result clearly shows that the amplification saturation is reached with sufficient input flux. The energy-extraction efficiency in the amplifier stage exceeded 18%, which is sufficient for practical use. Even at a 10-Hz operation, 100-mW average power after amplifier was obtained.

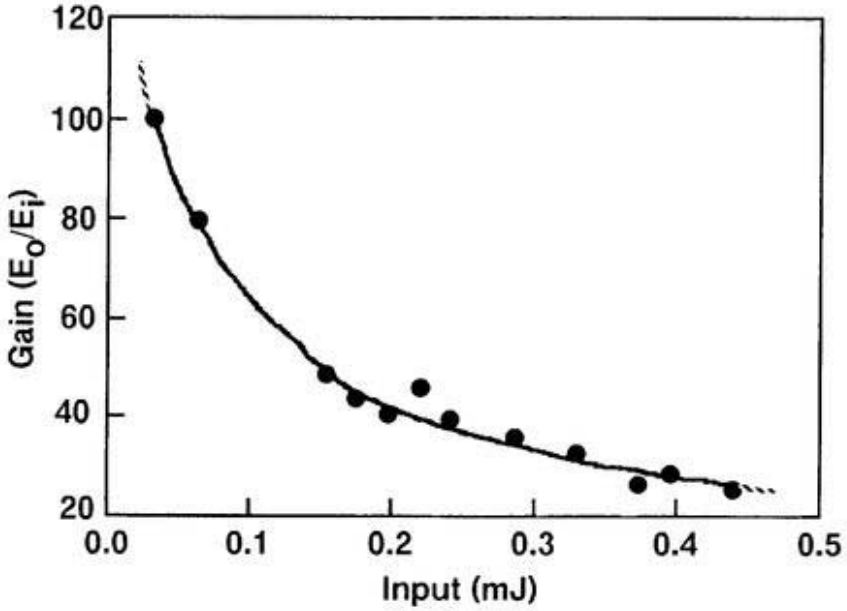

Fig. 4.5 Output gain dependence on input energy of the amplifier. This result clearly shows that the amplification saturation is reached with sufficient input flux.

Summary: We have demonstrated the direct generation and efficient amplification of UV short pulses from the simplest, all-solid-state, UV, short-pulse MOPA system composed of Ce:LiCAF crystals and conventional Q-switched Nd:YAG lasers. In this way, we have proven that the Ce:LiCAF-

based MOPA system is as effective and practical as other UV short-pulse systems.

Chapter 5. High-pulse-energy UV laser using large-size Ce:LiCAF crystal

** J. Crystal Growth **197**, 896-900 (1999).*

** Japanese J. of Applied Physics **37**, L1318-L1319 (1998).*

We have demonstrated a short-pulse (1 ns) Ce:LiCAF MOPA system. Due to the limited size of the available crystals, it was difficult to obtain a high energy output directly from a Ce:LiCAF laser. In this chapter, we present high-energy UV pulse generation from a Ce:LiCAF laser operating at 290 nm wavelength at a 10-Hz repetition rate using large-size Ce:LiCAF crystal.

5.1 Preparation of large-size Ce:LiCAF crystal [48]

The Ce:LiCAF crystal was grown in Tohoku University. Crystal growth was performed in a Czochralski system with automatic diameter control (ADC). A stoichiometric charge composed of commercially available high-purity (>99.99%) AlF_3, CaF_2 and LiF was used as the starting material. In the first growth, a Cr:LiCAF seed oriented along the a-axis was used. The charges were loaded in 40x40 mm^2 glassy carbon crucibles. The concentration of cerium in the starting material ranged from 1 to 2 mol%. In order to eliminate water and/or oxygen from the growth chamber, vacuum treatment was performed before the growth. After the vacuum treatment, the furnace was flushed with argon and the material was melted at 825°C. The applied growth rate was 0.7 mm/h and the rotation rate was 13 rpm. To prevent severe cracking of the boules, the furnace was cooled at a rate of 25°C/h. In this manner, a large Ce:LiCAF crystal of 15 mm diameter was grown successfully. Figure 5.1 shows a polished Ce:LiCAF wafer cut perpendicular to the growth axis. Grown crystals were free of cracks.

Fig. 5.1 Photograph of the large Czochralski-grown Ce:LiCAF crystal with 15-mm diameter.

5.2 High-energy pulse generation from a Ce:LiCAF oscillator [49]

The schematic diagram of a Ce:LiCAF laser resonator using the large-size Ce:LiCAF crystal is shown in Fig. 5.2. The laser resonator is established by a flat high reflector and a flat output coupler with 30% reflection for 290 nm and 75% transmission for 266 nm separated by 4 cm. The large Ce:LiCAF crystal grown by the method described above (18 mm in diameter, clear aperture 15 mm, length 10 mm) is doped with 1.2 mol% Ce^{3+} ions. There is no coating on the parallel end faces of the crystal that are perpendicular to the optical axis of

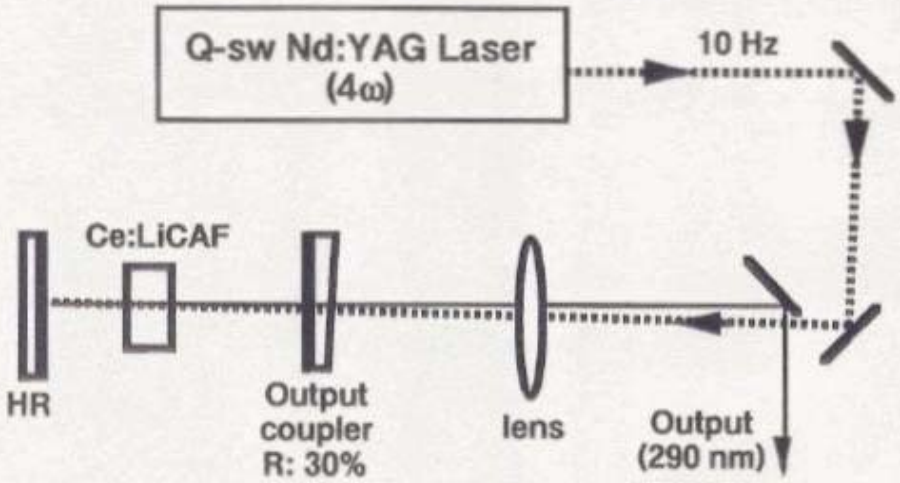

Fig. 5.2 Experimental setup of the Ce:LiCAF laser oscillator pumped by the fourth harmonic of a Q-switched Nd:YAG laser using a quasi-longitudinal pumping scheme.

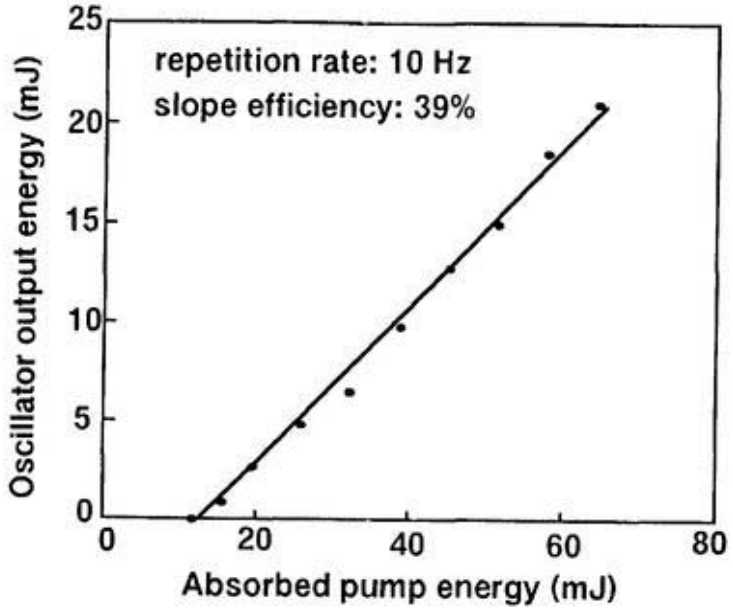

Fig. 5.3 Laser output energy as a function of absorbed pump energy. The measured output energy remained linear with pump fluence with a slope efficiency of 39%.

the resonator. The fourth harmonic of a Q-switched Nd:YAG laser is used as the pumping source. To obtain a high-quality laser beam, we used the quasi-longitudinal pumping method. Because it is difficult to fabricate an end mirror with high reflection for 290 nm and high transmission for 266 nm pump beams while maintaining a high damage threshold, we chose to pump the Ce:LiCAF crystal from the output-coupler side that has almost the same transmission for the pump and output wavelengths. To obtain high-energy output without damage to the crystal and optics in the cavity, a large pump beam cross section is necessary. The horizontally polarized pump beam is focused with a 40-cm-focal-length lens to produce a 4-mm-diameter spot at the surface of the Ce:LiCAF crystal without any damage to the crystal. To reduce the diffraction effects and disturbance to the beam uniformity, it is better to choose a ratio of crystal radius to beam radius as 2 or greater. Therefore, a much larger crystal diameter than the pump beam diameter is preferred. More than 85% of the incident pump pulse energy is absorbed by the crystal, so the crystal is long

enough for practical use. Figure 5.3 presents the obtained output energies at 290 nm as a function of the absorbed 266-nm pump energy. The laser oscillation threshold is 12 mJ, which corresponds to a threshold fluence of approximately 100 mJ/cm^2. The measured output energy remained linear with pump fluence with a slope efficiency of 39%. The efficiency can be improved by using a Brewster-cut crystal with antireflective coating. The highest pulse energy was 21 mJ at 10 Hz and 290 nm. The satellite-free single pulse with 3 ns duration was detected by a biplanar phototube as shown in Fig. 5.4.

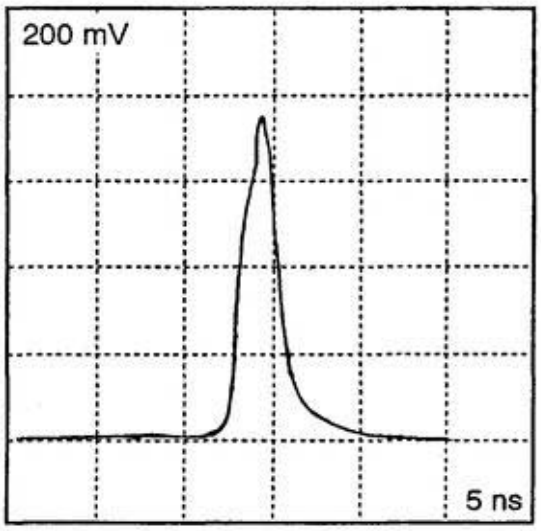

Fig. 5.4 Oscilloscope trace of the Ce:LiCAF laser output pulse. The satellite-free single pulse with 3 ns duration was detected by a biplanar phototube.

Because the loss of the pumping pulse energy through the output coupler was still large, a non-collinear pumping scheme was tried as shown in Fig 5.5. The large pumping beam cross section made it possible to achieve efficient pumping. The angle between the pumping beam and the output beam was about 5 degrees. The obtained output energies at 290 nm as a function of the absorbed 266-nm pump energy is shown in Fig. 5.6. In this case, the output pulse energy was improved up to 30.5 mJ, and the slope efficiency was also 39%.

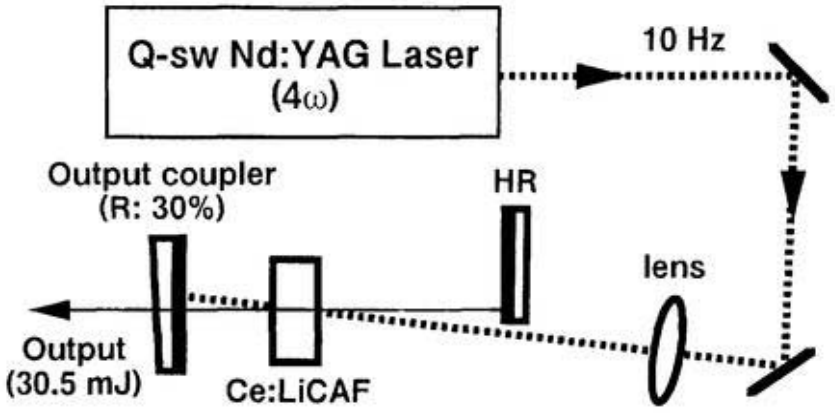

Fig. 5.5 Experimental setup of the Ce:LiCAF laser oscillator using a non-collinear pumping scheme.

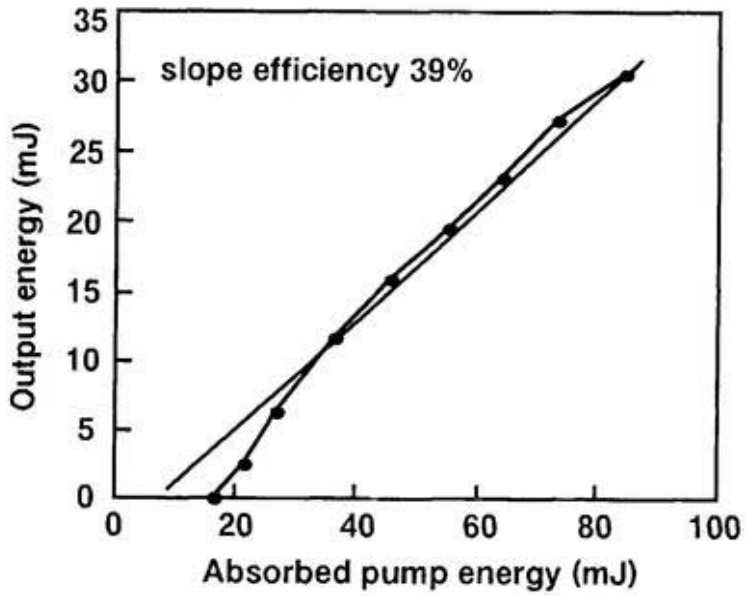

Fig. 5.6 Laser output energy as a function of absorbed pump energy. The output pulse energy was improved up to 30.5 mJ, and the slope efficiency was also 39%.

To demonstrate the tunability of the Ce:LiCAF laser consisting of the large-size Ce:LiCAF crystal, a grating was used as the tuning element, while acted as the end mirror of the oscillator as shown in Fig. 5.7. The grating worked in the Littrow condition. The incidence of the grating and its first order diffraction

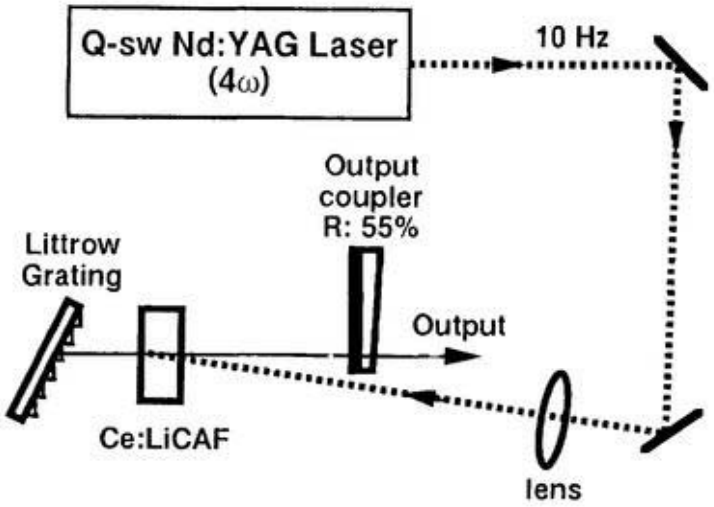

Fig. 5.7 Experimental setup of tunable Ce:LiCAF laser. A grating was used as the tuning element, while acted as the end mirror of the oscillator. The grating worked in the Littrow condition.

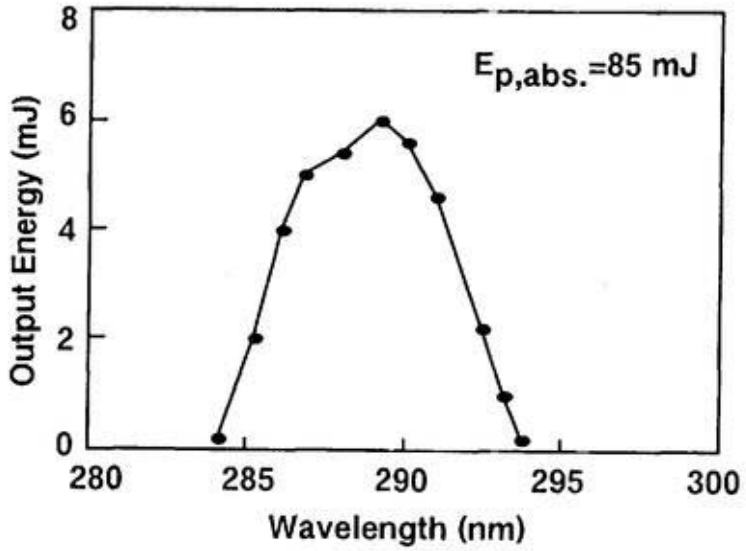

Fig. 5.8 Tuning curve for the tunable Ce:LiCAF laser. The limited tunable range was due to the low diffraction efficiency of the grating for the 290-nm wavelength.

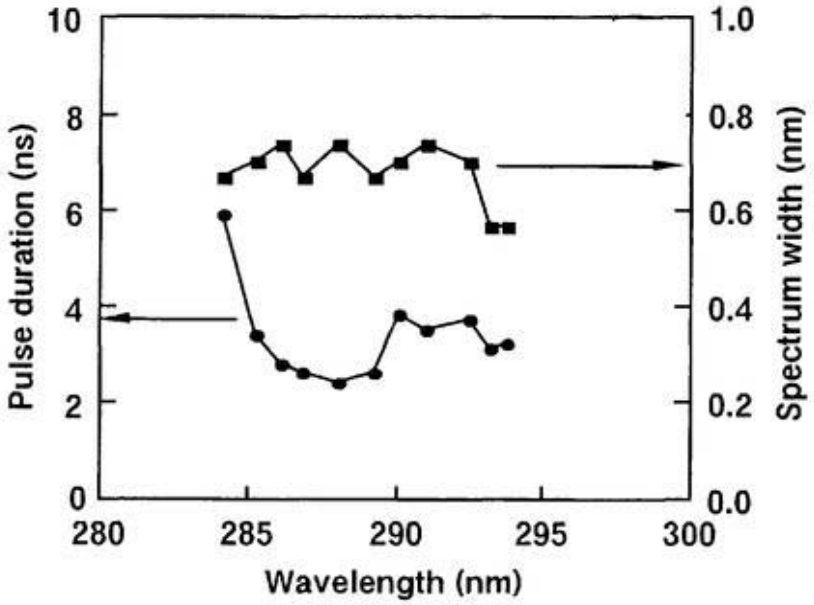

Fig. 5.9 Pulse widths and spectrum widths of the output pulses for different wavelengths. The pulse widths were around 4 ns, and the spectrum widths were about 0.7 nm.

overlapped. The grating used here was blazed for 500 nm wavelength. The obtained tuning range was from 284 nm to 294 nm as shown in Fig. 5.8, the maximum output was 6 mJ. The limited tunable range was due to the low diffraction efficiency of the grating for the 290-nm wavelength. A broader tunable range can be expected using a grating blazed for 290-nm wavelength. The pulse widths were around 4 ns, and the spectrum widths were about 0.7 nm (Fig. 5.9).

To generate pulses with much higher energy, the fourth harmonics of two simultaneous Q-switched Nd:YAG lasers were used as the pumping sources (Fig. 5.10). The three pump beams were focused with a 40-cm-focal-length lens to produce a spot size of ϕ 6 mm at the surface of the Ce:LiCAF crystal. With the total pumping energy of 230 mJ, the output pulse energy as high as 60 mJ was achieved at 290 nm at 10 Hz repetition rate, which is the highest performance reported for a Ce:LiCAF oscillator until now, as far as we know.

In this way, we demonstrated the generation of high-energy pulse at 290 nm very easily and efficiently.

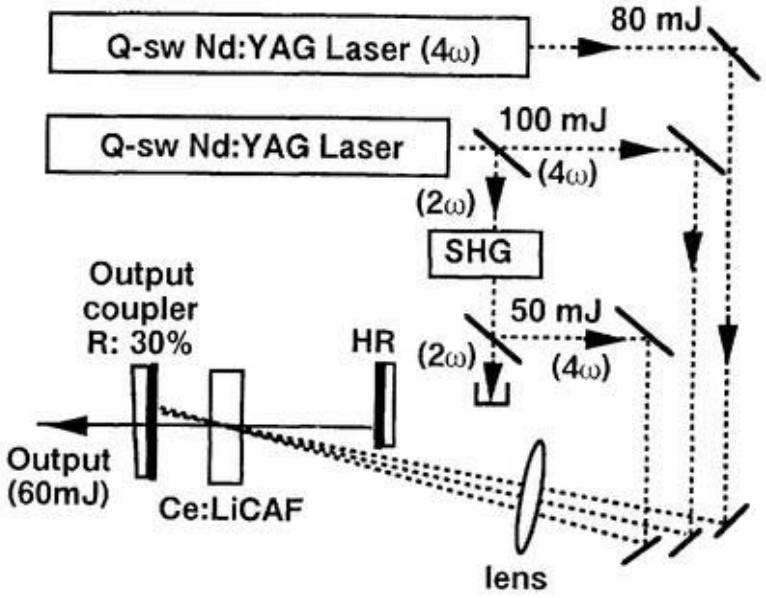

Fig. 5.10 Experimental setup of the Ce:LiCAF laser oscillator pumped by the fourth harmonics of two Q-switched Nd:YAG lasers. The pulse energy as high as 60 mJ was achieved at 290 nm at 10 Hz repetition rate.

Summary: Large-size Ce:LiCAF crystals with 15 mm diameter were grown successfully by the Czochralski method in Tohoku university. Due to the available large-size Ce:LiCAF crystal, 60-mJ output energy was obtained from the Ce:LiCAF laser pumped by the fourth harmonics of Q-switched Nd:YAG lasers. High slope efficiency of 39% was demonstrated. A much higher output can be expected by fully utilizing the crystal cross size while using a larger pumping source. This suggests that Ce:LiCAF is a promising material for high-energy ultraviolet pulse generation combined with high-power, Q-switched Nd:YAG lasers.

Chapter 6. Conclusions and prospects

As mentioned above, tunable lasers in the ultraviolet region with tunability centered around 290 nm are of special interest for applications relating to the remote sensing. The simple, compact, all-solid-state Ce:LiCAF (282-314 nm) laser can generate coherent radiation in this wavelength region. Ce:LLF has a potential longer-wavelength tuning region of around 305 to 340 nm, so it is especially attractive for use in spectroscopy of wide band-gap semiconductors for blue laser diodes, such as GaN. Their broad gain bandwidth corresponding to a few femtoseconds is extremely attractive for short-pulse applications.

The solid-state, tunable, ultraviolet crystals, Ce:LLF and Ce:LiCAF were proven to be very efficient and reliable to realize UV lasers. Subnanosecond ultraviolet coherent pulses were generated directly from solid-state lasers simply for the first time using low-Q, short-cavity Ce:fluoride lasers pumped by the fifth [39] and fourth [44] harmonics of Nd:YAG lasers.

To prove the tunability of these laser materials, we made a tunable all-solid-state Ce:LLF laser with the fifth harmonic of an Nd:YAG laser as the pumping source [39]. We also demonstrated a tunable Ce:LiCAF laser with broad tuning region from 282 nm to 314 nm [44]. Furthermore, we obtained tunable UV pulses around 230 nm by the sum-frequency mixing of Ce:LiCAF and Nd:YAG lasers [45].

We have demonstrated the direct generation and efficient amplification of UV short pulses from the simplest, all-solid-state, UV short-pulse, MOPA system composed of Ce:LiCAF crystals and conventional Q-switched Nd:YAG lasers [46]. In this way, we have proven that the Ce:LiCAF-based MOPA system is as effective and practical as other UV short-pulse systems.

Large-size Ce:LiCAF crystals with 15 mm diameter were grown successfully by the Czochralski method in Tohoku University recently [48]. Due to the available large Ce:LiCAF crystal, we have obtained 60-mJ output

energy from the Ce:LiCAF laser, the highest output directly from a Ce:LiCAF laser reported until now. A much higher output can be expected by fully utilizing the crystal cross size while using a larger pumping source. This suggests that Ce:LiCAF is a promising material for high-energy ultraviolet pulse generation combined with a high-power, Q-switched Nd:YAG laser [49].

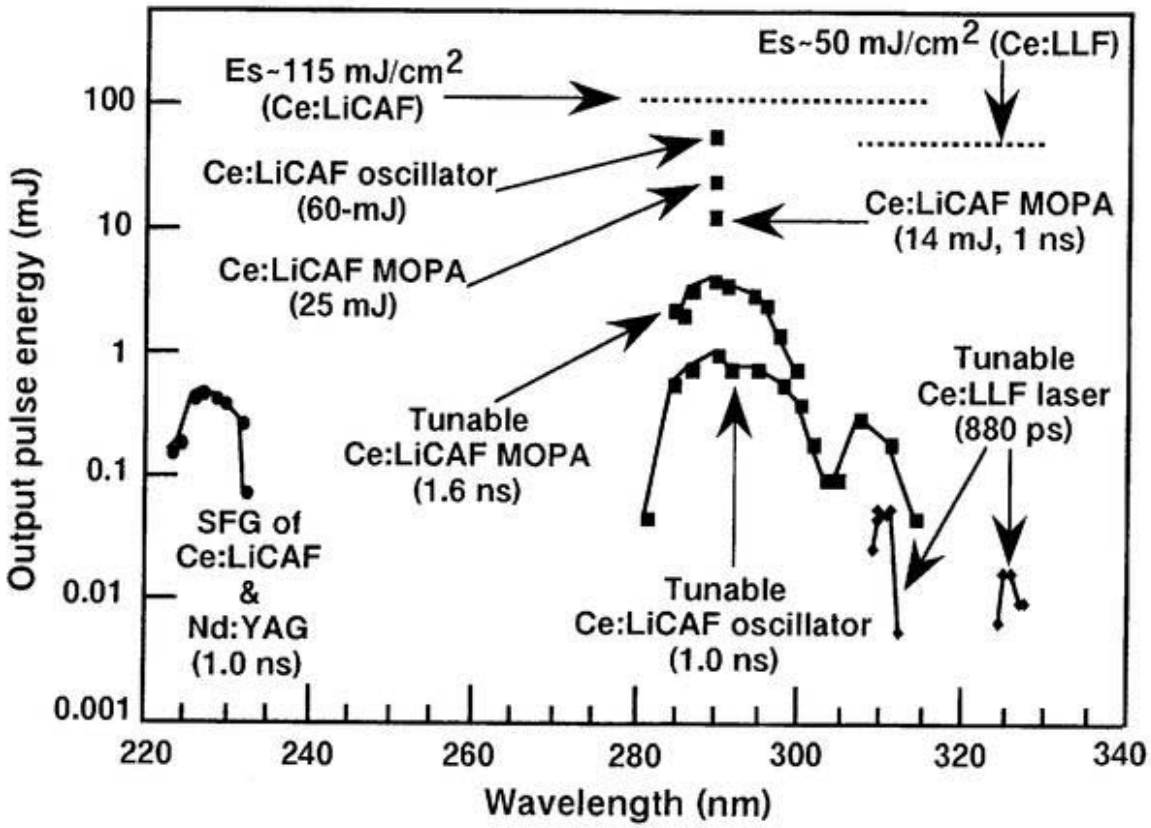

Fig. 6.1 Tuning curves for Ce^{3+} ions activated laser systems.

Ce:fluoride laser has been used to environmental sensing [50]. Narrow lasing linewidth (< 0.1 nm) operation was demonstrated in distributed-feedback, tunable Ce^{3+}-doped colquiriite lasers [51]. Ce:LiCAF laser worked efficiently at 20 kHz repetition rate [52]. Recently, a Ce:LiCAF laser pumped by the sum-frequency-mixing (271 nm) of the green and yellow fundamental lines (511 and 578 nm) from a copper-vapor laser was reported [53]. The basic optical properties of Ce^{3+} ions in both oxide and fluoride hosts were

investigated [54]. Especially, the room temperature fluorescence spectrum of Ce^{3+}-doped $LiBaF_3$ (Ce:LBF) spans the spectral region of 300-450 nm [55].

With the development of the UV laser media and nonlinear crystals, solid-state tunable ultraviolet short-pulse lasers have been realized as shown in Fig. 6.1 [41, 49]. It is reasonable to expect the cw solid-state ultraviolet lasers in future with the improvement of Ce:fluoride crystal qualities and high power ultraviolet cw pumping sources.

In conclusion of this thesis, we believe, with the improvement of the quality and size of UV laser crystals and nonlinear crystals (which are important for the cw UV pumping sources), all-solid-state, compact, ultrashort pulse, ultraviolet, tunable Ce:fluoride lasers will be possible in the near future. Further development of laser systems using these laser media will open up new possibility of simple and compact tunable UV ultrashort-pulse laser light sources.

References

[1] G. J. Megie, G. Ancellet, and J. Pelon, "Lidar measurements of ozone vertical profiles," Appl. Opt. **24**, 3454-3463 (1985).

[2] E. V. Browell, "Applications of lasers in remote sensing," in Advanced Solid-State Lasers, OSA Technical Digest, paper MA1, pp. 2-4 (1995).

[3] P. F. Moulton, "Spectroscopic and laser characteristics of Ti:Al_2O_3," J. Opt. Soc. Am. B **3**, 125-133 (1986).

[4] J. C. Walling, O. G. Peterson, H. P. Jenssen, R. C. Morris, and E. W. O'Dell, "Tunable alexandrite lasers," IEEE J. Quantum Electron. **QE-16**, 1302-1315 (1980).

[5] S. A. Payne, L. L. Chase, H. W. Newkirk, L. K. Smith, and W. F. Krupke, "$LiCaAlF_6:Cr^{3+}$: a promising new solid-state laser material," IEEE J. Quantum Electron. **24**, 2243-2252 (1988).

[6] S. A. Payne, L. L. Chase, L. K. Smith, W. L. Kway, and H. W. Newkirk, "Laser performance of $LiSrAlF_6:Cr^{3+}$," J. Appl. Phys. **66**, 1051-1056 (1989).

[7] W. L. Pryor, Laser Focus World: Buyers' Guide. Tulsa, OK: PennWell, 1994.

[8] J. F. Pinto, L. Esterowitz, and G. H. Rosenblatt, "Tunable UV source based on tripled Cr:LiSAF," in Advanced Solid-State Lasers, OSA Technical Digest, paper WD6, pp. 279-281 (1995).

[9] D. Strickland and G. Mourou, "Compression of amplified chirped optical pulses," Opt. Commun. **56**, 219-221 (1985).

[10] D. J. Ehrlich, P. F. Moulton, and R. M. Osgood, Jr., "Ultraviolet solid-state Ce:YLF laser at 325 nm," Opt. Lett. **4**, 184-186 (1979).

[11] D. J. Ehrlich, P. F. Moulton, and R. M. Osgood, Jr., "Optically pumped Ce:LaF_3 laser at 286 nm," Opt. Lett. **5**, 339-341 (1980).

[12] M. A. Dubinskii, R. Y. Abdulsabirov, S. L. Korableva, A. K. Naumov, and V. V. Semashko, "New solid-state active medium for tunable ultraviolet lasers," in 18th International Quantum Electronics Conference, OSA Technical Digest (Optical Society of America, Washington, DC, 1992), Paper FrL2, pp. 548-550.

[13] M. A. Dubinskii, R. Y. Abdulsabirov, S. L. Korableva, A. K. Naumov, and V. V. Semashko, "A new active medium for a tunable solid-state UV laser with an excimer pump," Laser Phys. **4**, 480-484 (1994).

[14] M. A. Dubinskii, V. V. Semashko, A. K. Naumov, R. Y. Abdulsabirov, and S.L. Korableva, "Active medium for all-solid-state tunable UV laser," OSA Proceedings on Advanced Solid-State Lasers, Albert A. Pinto and Tso Yee Fan,

eds. (Optical Society of America, Washington, DC, 1993), vol. 15, pp. 195-198.

[15] M. A. Dubinskii, V. V. Semashko, A. K. Naumov, R. Y. Abdulsabirov, and S. L. Korableva, "Spectroscopy of a new active medium of a solid-state UV laser with broadband single-pass gain," Laser Phys. **3**, 216-217 (1993).

[16] M. A. Dubinskii, V. V. Semashko, A. K. Naumov, R. Y. Abdulsabirov, and S. L. Korableva, "Ce^{3+}-doped colquiriite, a new concept of all-solid-state tunable ultraviolet laser," J. Mod. Opt. **40**, 1-5 (1993).

[17] J. F. Pinto, G. H. Rosenblatt, L. Esterowitz, and G. J. Quarles, "Tunable solid-state laser action in Ce^{3+}:$LiSrAlF_6$," Electron. Lett. **30**, 240-241 (1994).

[18] C. D. Marshall, S. A. Payne, J. A. Speth, W. F. Krupke, G. J. Quarles, V. Castillo, and B. H. T. Chai, "Ultraviolet laser emission properties of Ce^{3+} -doped $LiSrAlF_6$ and $LiCaAlF_6$," J. Opt. Soc. Am. B **11**, 2054-2065 (1994).

[19] K. H. Yang and J. A. Deluca, "UV fluorescence of cerium-doped lutetium and lanthanum trifluorides, potential tunable coherent sources from 2760 to 3220 A," Appl. Phys. Lett. **31**, 594-596 (1977).

[20] R. W. Waynant, "Vacuum ultraviolet laser emission from Nd^{+3}:LaF_3," Appl. Phys. B **28**, 205 (1982).

[21] W. J. Miniscalco, J. M. Pellegrino, and W. M. Yen, "Measurements of excited-state absorption in Ce^{3+}:YAG," J. Appl. Phys. **49**, 6109-6111 (1978).

[22] R. R. Jacobs, W. F. Krupke, and M. J. Weber, "Measurement of excited-state absorption loss for Ce^{3+} in $Y_3Al_5O_{12}$ and implications for 5d-4f rare-earth lasers," Appl. Phys. Lett. **33**, 410-412 (1978).

[23] D. S. Hamilton, "Trivalent cerium doped crystals as tunable system. Two bad apples," in *Tunable Solid State Lasers*, Berlin: Springer, 1985, pp. 80-90.

[24] Ki-Soo Lim and D. S. Hamilton, "Optical gain and loss studies in Ce^{3+}:$YLiF_4$," J. Opt. Soc. Am. B **6**, 1401-1406 (1989).

[25] K. S. Lim and D. S. Hamilton, "UV-induced loss mechanisms in a Ce^{3+}:$YLiF_4$ laser," J. Luminescence **40 & 41**, 319-320 (1988).

[26] J. F. Owen, P. B. Dorain, and T. Kobayasi, "Excited-state absorption in Eu^{2+}:CaF_2 and Ce^{3+}:YAG single crystals at 298 and 77 K," J. Appl. Phys. **52**, 1216-1223 (1981).

[27] D. S. Hamilton, S. K. Gayen, G. J. Pogatshnik, and R. D. Ghen, "Optical-absorption and photoionization measurements from the excited states of Ce^{3+}:$Y_3Al_5O_{12}$," Phys. Rev. B **39**, 8807-8815 (1989).

[28] G. J. Pogatshnik and D. S. Hamilton, "Excited-state photoionization of Ce^{3+} ions in

Ce^{3+}:CaF_2," Phys. Rev. B **36**, 8251-8257 (1987).

[29] M. A. Dubinskii, A. C. Cefalas, E. Sarantopoulou, S. M. Spyrou, C. A. Nicolaides, R. Y. Abdulsabirov, S. L. Korableva, and V. V. Semashko, "Efficient LaF_3:Nd^{3+}-based vacuum-ultraviolet laser at 172 nm," J. Opt. Soc. Am. B **9**, 1148-1150 (1992).

[30] S. Nakamura, M. Senoh, S. Nagahama, N. Iwasa, T. Yamada, T. Matsushita, Y. Sugimoto, and H. Kiyoku, "Continuous-wave operation of InGaN multi-quantum-well-structure laser diodes at 233 K," Appl. Phys. Lett. **69**, 3034-3036 (1996).

[31] N. Sarukura, Z. Liu, Y. Segawa, K. Edamatsu, Y. Suzuki, T. Itoh, V. V. Semashko, A. K. Naumov, S. L. Korableva, R. Y. Abdulsabirov, and M. A. Dubinskii, "Ce^{3+}:$LiLuF_4$ as a broad band ultraviolet amplification medium", Opt. Lett. **20**, 294-296 (1995).

[32] R. Y. Abdulsabirov, M. A. Dubinskii, and B. N. Kazakov, Sov. Phys. Crystallogr. **32**, 559 (1987).

[33] L. M. Frantz and J. S. Nodvick, "Theory of pulse propagation in a laser amplifier," J. Appl. Phys. **34**, 2346-2349 (1963).

[34] N. Sarukura, M. A. Dubinskii, Z. Liu, V. V. Semashko, A. K. Naumov, S. L. Korableva, R. Yu. Abdulsabirov, K. Edamatsu, Y. Suzuki, T. Itoh, and Y. Segawa, "Ce^{3+} activated fluoride crystals as prospective active media for widely tunable ultraviolet ultrafast lasers with direct 10-nsec pumping", IEEE J. of Selected Topics in Quantum Electron. **1**, 792-804 (1995).

[35] For example; D. E. Spence, P. N. Kean, and W. Sibbett, "60-fsec pulse generation from a self-mode-locked Ti:sapphire laser," Opt. Lett. **16**, 42-44 (1991).

[36] For example; N. Sarukura, Y. Ishida, and H. Nakano, "Generation of 50-fsec pulses from a pulse-compressed, cw, passively mode-locked Ti:sapphire laser," Opt. Lett. **16**, 153-155 (1991).

[37] C. Lin and C. V. Shank, "Subnanosecond tunable dye laser pulse generation by controlled resonator transients," Appl. Phys. Lett. **26**, 389-391 (1975).

[38] D. Roess, "Giant pulse shortening by resonator transients," J. Appl. Phys. **37**, 2004-2006 (1966).

[39] N. Sarukura, Z. Liu, S. Izumida, M. A. Dubinskii, R. Y. Abdulsabirov, and S. L. Korableva, "All-solid-state tunable ultraviolet sub-nanosecond laser with direct pumping by the fifth harmonic of an Nd:YAG laser," Appl. Opt. **37**, 6446-6448 (1998).

[40] Y. Mori, S. Nakajima, A. Taguchi, A. Miyamoto, M. Inakaki, W. Zhou, T. Sasaki,

and S. Nakai, "Nonlinear optical properties of cesium lithium borate," Jpn. J. Appl. Phys. **34**, L296-L298 (1995).

[41] R. Komatsu, T. Sugawara, K. Sassa, N. Sarukura, Z. Liu, S. Izumida, S. Uda, T. Fukuda, and K. Yamanouchi, "Growth and ultraviolet application of $Li_2B_4O_7$ crystals: generation of the fourth harmonic and fifth harmonics of Nd:$Y_3Al_5O_{12}$ lasers", Appl. Phys. Lett. **70**, 3492-3494 (1997).

[42] Z. Liu, N. Sarukura, M. A. Dubinskii, R. Y. Abdulsabirov, and S. L. Korableva, "All-solid-state subnanosecond tunable ultraviolet laser sources based on Ce^{3+}-activated fluoride crystals", J. of Nonlinear Optical Physics and Materials **8**, 41-54 (1999).

[43] P. F. Moulton, "Tunable paramagnetic-ion lasers," in Laser Handbook, edited by M. Bass and M. L. Stitch (Elseviers Science Publishers B.V., 1985), p. 284.

[44] Z. Liu, H. Ohtake, N. Sarukura, M. A. Dubinskii, R. Y. Abdulsabirov, S. L. Korableva, A. K. Naumov, and V. V. Semashko, "Subnanosecond tunable ultraviolet pulse generation from a low-Q, short-cavity Ce:LiCAF laser", Jpn. J. Appl. Phys. **36**, L1384-L1386 (1997).

[45] Z. Liu, N. Sarukura, M. A. Dubinskii, R. Y. Abdulsabirov, S. L. Korableva, A. K. Naumov, and V. V. Semashko, "Tunable ultraviolet short-pulse generation from a Ce:LiCAF laser amplifier system and its sum-frequency mixing with an Nd:YAG laser", Jpn. J. Appl. Phys. **37**, L36-L38 (1998).

[46] N. Sarukura, Z. Liu, H. Ohtake, Y. Segawa, M. A. Dubinskii, R. Y. Abdulsabirov, S. L. Korableva, A. K. Naumov, and V. V. Semashko, "Ultraviolet short pulses from an all-solid-state Ce:LiCAF master oscillator and power amplifier system", Opt. Lett. **22**, 994-996 (1997).

[47] N. Sarukura and Y. Ishida, "Ultrashort pulse generation from a passively mode-locked Ti:sapphire laser based system," IEEE J. Quantum Electron. **28**, 2134-2141 (1992).

[48] K. Shimamura, N. Mujilatu, K. Nakano, S. L. Baldochi, Z. Liu, H. Ohtake, N. Sarukura, and T. Fukuda, "Growth and characterization of Ce-doped $LiCaAlF_6$ single crystals", J. Crystal Growth **197**, 896-900 (1999).

[49] Z. Liu, S. Izumida, H. Ohtake, N. Sarukura, K. Shimamura, N. Mujilatu, S. L. Baldochi, and T. Fukuda, "High-pulse-energy, all-solid-state, ultraviolet laser oscillator using large Czochralski-grown Ce:LiCAF crystal," Jpn. J. Appl. Phys. **37**, L1318-L1319 (1998).

[50] P. Rambaldi, M. Douard, J. -P. Wolf, "New UV tunable solid-state lasers for lidar applications," Appl. Phys. B **61**, 117-120 (1995).

[51] J. F. Pinto and L. Esterowitz, "Distributed-feedback, tunable Ce^{3+}-doped colquiriite

lasers," Appl. Phys. Lett. **71**, 205-207 (1997).

[52] A. B. Petersen, "All solid-state, 228-240 nm source based on Ce:LiCAF," Advanced Solid-State Lasers '97 (OSA), paper PD2 (1997).

[53] A. J. S. McGonigle, D. W. Coutts, and C. E. Webb, "530-mW 7-kHz cerium LiCAF laser pumped by the sum-frequency-mixed output of a copper-vapor laser," Opt. Lett. **24**, 232-234 (1999).

[54] D. A. Hammons, M. C. Richardson, B. H. T. Chai, and M. Bass, "Spectroscopic properties of Ce^{3+} in orthosilicate, garnet, and fluoride crystals," OSA Trends in Optics and Photonics (Optical Society of America), Vol. 10, Advanced Solid State Lasers, pp. 35 (1997).

[55] M. A. Dubinskii, K. L. Schepler, V. V. Semashko, R. Yu. Abdulsabirov, B. M. Galjautdinov, S. L. Korableva, and A. K. Naumov, "Ce^{3+}:$LiBaF_3$ as new prospective active material for tunable UV laser with direct UV pumping," OSA Trends in Optics and Photonics (Optical Society of America), Vol. 10, Advanced Solid State Lasers, pp. 30 (1997).

Acknowledgment

The author would like to express sincere gratitude to Associate Prof. N. Sarukura for science guidance throughout the study and for providing a chance of studying and working in The Graduate University for Advanced Studies and Institute for Molecular Science.

The author would like to thank to Dr. M. A. Dubinskii in Science & Engineering Services, Inc. of America for useful discussions and for providing various Ce-doped crystals.

The author would like to thank to Dr. Y. Segawa in the Photodynamics Research Center of The Institute of Physical and Chemical Research and Prof. T. Itoh in Tohoku University for their continuous encouragement and helpful discussions.

The author is grateful to Dr. K. Shimamura and Prof. T. Fukuda in Tohoku University for useful discussions and providing Ce:LiCAF crystals.

The author wishes to thank to Mr. S. Izumida, Mr. S. Ono, and Dr. H. Ohtake in Institute for Molecular Science for their excellent assistance in the experiments and for helpful discussions.

Award and Publication List

Award: Excellent Presentation Award of the Laser Society of Japan in 1998.

Publication In Journal:

J-1 Z. Liu, N. Sarukura, M. A. Dubinskii, R. Y. Abdulsabirov, and S. L. Korableva,
"All-solid-state subnanosecond tunable ultraviolet laser sources based on Ce^{3+}-activated fluoride crystals",
J. of Nonlinear Optical Physics and Materials **8**, 41-54 (1999).

J-2 K. Shimamura, N. Mujilatu, K. Nakano, S. L. Baldochi, Z. Liu, H. Ohtake, N. Sarukura, and T. Fukuda,
"Growth and characterization of Ce-doped $LiCaAlF_6$ single crystals",
J. Crystal Growth **197**, 896-900 (1999).

J-3 Z. Liu, S. Izumida, H. Ohtake, N. Sarukura, K. Shimamura, N. Mujilatu, S. L. Baldochi, and T. Fukuda,
"High-pulse-energy, all-solid-state, ultraviolet laser oscillator using large Czochralski-grown Ce:LiCAF crystal,"
Jpn. J. Appl. Phys. **37**, L1318-L1319 (1998).

J-4 N. Sarukura, Z. Liu, S. Izumida, M. A. Dubinskii, R. Y. Abdulsabirov,
and S. L. Korableva,
"All-solid-state tunable ultraviolet sub-nanosecond laser with direct pumping by the fifth harmonic of an Nd:YAG laser,"
Appl. Opt. **37**, 6446-6448 (1998).

J-5 Z. Liu, N. Sarukura, M. A. Dubinskii, R. Y. Abdulsabirov, S. L. Korableva,
A. K. Naumov, and V. V. Semashko,
"Tunable ultraviolet short-pulse generation from a Ce:LiCAF laser amplifier system and its sum-frequency mixing with an Nd:YAG laser",
Jpn. J. Appl. Phys. **37**, L36-L38 (1998).

J-6 Z. Liu, H. Ohtake, N. Sarukura, M. A. Dubinskii, R. Y. Abdulsabirov, S. L. Korableva,
A. K. Naumov, and V. V. Semashko,
"Subnanosecond tunable ultraviolet pulse generation from a low-Q, short-cavity Ce:LiCAF laser",
Jpn. J. Appl. Phys. **36**, L1384-L1386 (1997).

J-7 N. Sarukura, Z. Liu, H. Ohtake, Y. Segawa, M. A. Dubinskii, R. Y. Abdulsabirov,

S. L. Korableva, A. K. Naumov, and V. V. Semashko,

"Ultraviolet short pulses from an all-solid-state Ce:LiCAF master oscillator and power amplifier system",

Opt. Lett. **22**, 994-996 (1997).

J-8 R. Komatsu, T. Sugawara, K. Sassa, N. Sarukura, Z. Liu, S. Izumida, Y. Segawa, S. Uda, T. Fukuda, and K. Yamanouchi,

"Growth and ultraviolet application of $Li_2B_4O_7$ crystals: generation of the fourth harmonic and fifth harmonics of Nd:$Y_3Al_5O_{12}$ lasers",

Appl. Phys. Lett. **70**, 3492-3494 (1997).

International Conference:

P-1. Z. Liu, S. Izumida, S. Ono, H. Ohtake, N. Sarukura, K. Shimamura, N. Mujilatu, S. L. Baldochi, and T. Fukuda,

"Direct generation of 30-mJ, 289-nm pulses from a Ce:LiCAF oscillator using Czochralski-grown large crystal",

Advanced Solid-State Lasers (Optical Society of America), paper TuB14, 1999.

P-2. Z. Liu, H. Ohtake, N. Sarukura, M. A. Dubinskii, R. Y. Abdulsabirov, and S. L. Korableva,

"All-solid-state tunable ultraviolet picosecond Ce^{3+}:$LiLuF_4$ laser with direct pumping by the fifth harmonic of a Nd:YAG laser",

OSA Trends in Optics and Photonics (Optical Society of America), vol. 19, Advanced Solid-State Lasers, 13-15 (1998).

P-3 Z. Liu, S. Izumida, S. Ono, H. Ohtake, N. Sarukura, K. Shimamura, Na Mujilatu, S. L. Baldochi, and T. Fukkuda,

"30-mJ pulse from ultraviolet laser oscillator using large Czochralski-grown Ce:LiCAF crystal,"

OSA Annual Meeting 1998 (Optical Society of America), paper PD11.

P-4. Z. Liu, H. Ohtake, S. Shinji, T. Yamanaka, N. Sarukura, M. A. Dubinskii, R. Y. Abdulsabirov, S. L. Korableva,

"All-solid-state tunable ultraviolet Ce activated fluoride laser systems directly pumped by the fourth and fifth harmonic of Nd:YAG lasers,"

Nonlinear Optics (IEEE/LEOS), Hawaii, August 10-14, 1998, paper ThC7.

P-5. Z. Liu, H. Ohtake, S. Shinji, T. Yamanaka, N. Sarukura, M. A. Dubinskii, R. Y. Abdulsabirov, S. L. Korableva,

"All-solid-state UV tunable picosecond Ce^{3+}:$LiLuF_4$ laser pumped at 213 nm," Conference on Lasers and Electro-Optics (Optical Society of America, 1998), paper CWF40.

P-6. Z. Liu, H. Ohtake, N. Sarukura, M. A. Dubinskii, R. Y. Abdulsabirov, S. L. Korableva, "All-solid-state tunable ultraviolet Ce activated fluoride laser systems directly pumped by the fourth and fifth harmonic of Nd:YAG lasers,"
1998 International Photonics Conference, paper F-PO29, Dec. 15, 1998, Taipei.

P-7. Z. Liu, N. Sarukura, H. Ohtake, S. Shinji, Y. Segawa, M. A. Dubinskii, R. Y. Abdulsabirov, S. L. Korableva, A. K. Naumov, and V. V. Semashko, "14-mJ, 1-nsec, 289-nm pulses from an all-solid-state Ce:LiCAF master oscillator and power amplifier system",
OSA Trends in Optics and Photonics (Optical Society of America), Vol. 10, Advanced Solid State Lasers, pp. 24 (1997).

P-8. Z. Liu, H. Ohtake, S. Izumida, N. Sarukura, M. A. Dubinskii, R. Y. Abdulsabirov, S. L. Korableva, A. K. Naumov, and V. V. Semashko,
"Ultraviolet tunable short pulses from an all-solid-state Ce:LiCAF master oscillator and power amplifier system",
Ultrafast Optics (IEEE), Monterey, California, USA, August 4-7, 1997, paper TP-22.

P-9. Z. Liu, H. Ohtake, N. Sarukura, M. A. Dubinskii, R. Y. Abdulsabirov, S. L. Korableva, A. K. Naumov, and V. V. Semashko,
"14-mJ short UV pulses from an all-solid-state Ce:LiCAF master oscillator and power amplifier system",
OSA Annual Meeting (Optical Society of America), paper MH2, 1997.

Domestic Conference:

C-1. Z. Liu, H. Ohtake, N. Sarukura, K. Shimamura, N. Mujilatu, and T. Fukuda,
"Direct generation of 60-mJ, 289-nm pulses from a Ce:LiCAF oscillator",
The 46th Spring Meeting of Japan Society of Applied Physics and Related Societies, 1999, paper 30a-YF-8.

C-2. Z. Liu, H. Ohtake, N. Sarukura, K. Shimamura, N. Mujilatu, and T. Fukuda,
"30-mJ pulse from ultraviolet laser oscillator using large Czochralski-grown Ce:LiCAF crystal",
The 19th Annual Meeting of the Laser Society of Japan, 1999, paper 28aI9.

C-3. Z. Liu, H. Ohtake, N. Sarukura, M. A. Dubinskii, R. Y. Abdulsabirov, and S. L. Korableva,
"High-power tunable ultraviolet pulse generation from a Ce:LiCAF MOPA system",
The 59th Autumn Meeting of Japan Society of Applied Physics, 1998, paper 17pV17.

C-4. Z. Liu, H. Ohtake, N. Sarukura, K. Shimamura, N. Mujilatu, and T. Fukuda,
"Efficient, high output energy, ultraviolet Ce:LiCAF laser",
The 59th Autumn Meeting of Japan Society of Applied Physics, 1998, paper 17pV16.

C-5. Z. Liu, H. Ohtake, N. Sarukura, M. A. Dubinskii, R. Y. Abdulsabirov, and S. L. Korableva,
"All-solid-state tunable ultraviolet picosecond Ce^{3+}:$LuLiF_4$ laser pumped by the fifth harmonic of an Nd:YAG laser",
The 45th Spring Meeting of Japan Society of Applied Physics and Related Societies, 1998, paper 28p-X-9.

C-6. Z. Liu, H. Ohtake, S. Izumida, T. Yamanaka, N. Sarukura, M. A. Dubinskii, R. Y. Abdulsabirov, S. L. Korableva, A. K. Naumov, and V. V. Semashko,
"All-solid-state tunable ultraviolet picosecond Ce:$LuLiF_4$ laser",
The 18th Annual Meeting of the Laser Society of Japan, 1998, paper 23pI10.

C-7. Z. Liu, H. Ohtake, N. Sarukura, M. A. Dubinskii, R. Y. Abdulsabirov, S. L. Korableva, A. K. Naumov, and V. V. Semashko,
"Tunable Ultraviolet Short-Pulse Generation from a Ce:LiCAF master oscillator and power amplifier system",
The 18th Annual Meeting of the Laser Society of Japan, 1998, paper 23pI9.

C-8. Z. Liu, H. Ohtake, N. Sarukura, M. A. Dubinskii, R. Y. Abdulsabirov, S. L. Korableva, A. K. Naumov, and V. V. Semashko,
"Tunable ultraviolet short pulse generation from a low-Q, short-cavity Ce:LiCAF laser",
The 58th Autumn Meeting of Japan Society of Applied Physics, 1997, paper 3a-PA-8.

C-9. Z. Liu, N. Sarukura, H. Ohtake, S. Shinji, Y. Segawa, M. A. Dubinskii, R. Y. Abdulsabirov, S. L. Korableva, A. K. Naumov, and V. V. Semashko,
"14-mJ pulses from an all-solid-state Ce:LiCAF master oscillator and power amplifier system",
The 44th Spring Meeting of Japan Society of Applied Physics and Related Societies, 1997, paper 30p-NB-2.

Other publication and presentation list

O-1. Z. Liu, S. Izumida, S. Ono, H. Ohtake, N. Sarukura,
"High-repetition-rate, high-average-power mode-locked Ti:sapphire laser with an intracavity cw-amplification scheme",
Appl. Phys. Lett. 74, 3622 (1999).

O-2. S. Izumida, S. Ono, Z. Liu, H. Ohtake, N. Sarukura,
"Spectrum control of THz radiation from InAs in a magnetic field by duration and frequency chirp of the excitation pulses",
Appl. Phys. Lett. 75, 451 (1999).

O-3. N. Sarukura, H. Ohtake, S. Izumida, and Z. Liu,
"High average-power THz-radiation from femtosecond laser-irradiated InAs in a magnetic field and its elliptical polarization characteristics,"
J. Appl. Phys. 84, 654 (1998).

O-4. N. Sarukura, H. Ohtake, Z. Liu, T. Itatani, T. Sugaya, T. Nakagawa, and Y. Sugiyama,
"THz-radiation generation from an intracavity saturable Bragg reflector in a magnetic field",
Jpn. J. Appl. Phys. 37, L125 (1998).

O-5. N. Sarukura, Z. Liu, H. Ohtake, S. Izumida, T. Yamanaka, Y. Segawa, T. Itatani, T. Sugaya, T. Nakagawa, and Y. Sugiyama,
"All-Solid-State, THz Radiation Source Using a Saturable Bragg Reflector in a Femtosecond Mode-Locked Laser",
Jpn. J. Appl. Phys. 36, L560 (1997).

O-6. Z. Liu, S. Izumida, S. Ono, H. Ohtake, and N. Sarukura,
"Spectrum control of coherent, short-pulse, far-infrared radiation from InAs under magnetic field irradiated with stretched femtosecond laser pulses",
Advanced Solid-State Lasers (Optical Society of America), 1999, paper ME13.

O-7. Z. Liu, S. Izumida, S. Ono, H. Ohtake, and N. Sarukura,
"High-average power mode-locked Ti:sapphire laser with newly-invented intra-cavity cw-amplification scheme",
Advanced Solid-State Lasers (Optical Society of America), 1999, paper PD16.

O-8. Z. Liu, H. Ohtake, S. Izumida, S. Ono, and N. Sarukura,
"Sub-mW, short-pulse THz-radiation from femtosecond-laser irradiated InAs and its polarization and spatial properties",
OSA Trends in Optics and Photonics (Optical Society of America), vol. 19, Advanced

Solid-State Lasers, 370-373 (1998).

O-9.Z. Liu, S. Izumida, S. Ono, H. Ohtake, and N. Sarukura,

"High-average power mode-locked Ti:sapphire laser with newly-invented intra-cavity cw-amplification scheme",

The 46th Spring Meeting of Japan Society of Applied Physics and Related Societies, 1999, paper 28p-C-4.

O-10. Z. Liu, H. Ohtake, N. Sarukura, A. Nishimura, and H. Takuma,

"Broad-band gain demonstration of new Yb:glass",

The 59th Autumn Meeting of Japan Society of Applied Physics, 1998, paper 17pV7.

O-11. Z. Liu, H. Ohtake, S. Izumida, T. Yamanaka, and N. Sarukura,

"High average power THz-radiation from femtosecond laser irradiated InAs under the magnetic field",

The 58th Autumn Meeting of Japan Society of Applied Physics, 1997, paper 3a-Z-9.